SALAMANDRA **50**(3) | 155–171 | 30 October 2014 | ISSN 0036–3375

Morphological variation and phylogeography of frogs related to *Pristimantis caryophyllaceus* (Anura: Terrarana: Craugastoridae) in Panama

Abel Batista[1,2], Andreas Hertz[1,2], Gunther Köhler[1], Konrad Mebert[3] & Milan Vesely[4]

[1)] Senckenberg Forschungsinstitut und Naturmuseum Frankfurt, Senckenberganlage 25, 60325 Frankfurt am Main, Germany

[2)] Goethe-University, Institute for Ecology, Evolution & Diversity, Biologicum, Building C, Max-von-Laue-Str. 13, 60438 Frankfurt am Main, Germany

[3)] Department of Environmental Sciences, Section of Conservation Biology, University of Basel, St. Johanns-Vorstadt 10, 4056 Basel, Switzerland

[4)] Department of Zoology, Faculty of Natural Sciences, Palacký University, 17. Listopadu 50, 77146 Olomouc, Czech Republic

Corresponding author: Abel Batista, e-mail: abelbatista@hotmail.com

Manuscript received: 4 November 2013

Accepted: 23 April 2014 by Jörn Köhler

Abstract. New World direct-developing frogs (Terrarana) are among the most diverse vertebrate groups in the world. Many Terrarana species are highly variable in colouration and morphology, often rendering it difficult to delineate species. Modern molecular and bioacoustic techniques are a relatively recent tool for understanding the various taxonomic entities. This affects also *Pristimantis caryophyllaceus,* a complex on which little research has previously been done. We examined the variation of morphology, genetics, and colouration in specimens affiliated to *P. caryophyllaceus* from Panama, using different Molecular Operational Taxonomic Units (MOTUs) based on molecular phylogenetic lineages. Phylogeny, ecology, and distributional information for this species shed light on the position and species delineation of *P. caryophyllaceus* and its congeners in Panama. Our results demonstrate a high level of genetic diversity in *P. caryophyllaceus*-like populations from Panama, which in fact comprise three main lineages that are geographically separated. Specimens from eastern Panama tend to be larger, with more expanded finger disks and toe pads than specimens from western Panama. However, aside from the significant morphological differences between MOTUs, the extent of variation within each MOTU is very large. Based on our extensive and integrative analysis, we suggest treating the three MOTUs of *P. caryophyllaceus* populations as a single polymorphic species with very deep conspecific lineages as a result of the dynamic geological history of the Isthmus of Panama. The validity of the recently described *P. educatoris* is not supported by our results and we therefore synonymize it with *P. caryophyllaceus*.

Key words. Amphibia, Anura, *Pristimantis caryophyllaceus*, *P. educatoris*, Panama, genetic variation, polymorphism, biogeography.

Introduction

Pristimantis caryophyllaceus (Barbour, 1928) is a widely distributed species that inhabits lowland, premontane and the lower portions of the lower montane forest domains, from Costa Rica through Panama to northwestern Colombia (Lynch 1980, Savage 2002). Although this species is distributed from sea level to 1,968 m above, it appears to be most common in the range from 300 to 1,600 m a.s.l. *Pristimantis caryophyllaceus* is characterized by a sharply projecting snout, a large and pointed heel tubercle, and a well-developed superciliary tubercle (Barbour 1928, Savage 2002). *Pristimantis caryophyllaceus* also exhibits a remarkable polychromatism and polymorphism (Hoffman & Blouin 2000, Savage 2002). Recently, one seemingly morphologically distinct lineage was described as a separate species, *P. educatoris,* by Ryan et al. (2010). These authors suggested that *P. educatoris* and *P. caryophyllaceus* are parapatric, with *P. caryophyllaceus* being distributed throughout Costa Rica and western Panama whereas *P. educatoris* occurs from west-central to eastern Panama and into Colombia. As the demarcation line separating the two taxa, these authors identified the high-altitude valley of the Río Chiriquí in the Fortuna depression. However, Ryan et al. (2010) also identified a disjunctive population of *P. educatoris* in extreme southeastern Costa Rica based on two specimens, contradicting this biogeographical concept. Moreover, the morphological analysis and description of *P. educatoris* is based only on specimens from the type locality (i.e., El Copé, Coclé, Panama; Ryan et al. 2010).

Recent genetic studies identified three deep genetic lineages with up to 14.5% divergence (Kimura 2-parameter distance) in the mitochondrial COI gene between samples of *P. caryophyllaceus* from Costa Rica, central Panama, and eastern Panama, respectively (Crawford et al. 2010, Pinto-Sánchez et al. 2012). Crawford et al. (2010) contemplated a possible co-occurrence of at least three candidate species that were concealed under the name *P. caryophyllaceus* at El Copé (Crawford et al. 2010). *Pristimantis caryophyllaceus* is indeed an old lineage, which originated in South America about 12 million years ago and subsequently evolved and expanded its range into Central America prior to the closure of the Isthmus of Panama (Pinto-Sánchez et al. 2012). As a consequence, the divergence of different lineages was triggered by the dynamic geological history in the region and the rise of the Isthmus of Panama, which ultimately resulted in various isolation processes over time.

Ecological information on *Pristimantis caryophyllaceus* (sensu lato) (Dunn 1937, Miyamoto 1984, Heinen 1992, Savage 2002, Lips et al. 2003) is mostly available on populations from western Panama and eastern Costa Rica, whereas there is only little information on the natural history of eastern Panamanian or Colombian populations (Myers 1969). Herein, we contribute new information by describing for the first time the advertisement call of *P. caryophyllaceus* from eastern Panama, and providing additional data on its ecology, biogeography and morphology in an integrative taxonomic approach to potential species delineation within the *P. caryophyllaceus* complex in Panama.

Materials and methods

Fieldwork was carried out in the mountain ranges of Darién, Jingurudó, Majé, Pirre, San Blas, and Sapo in east-

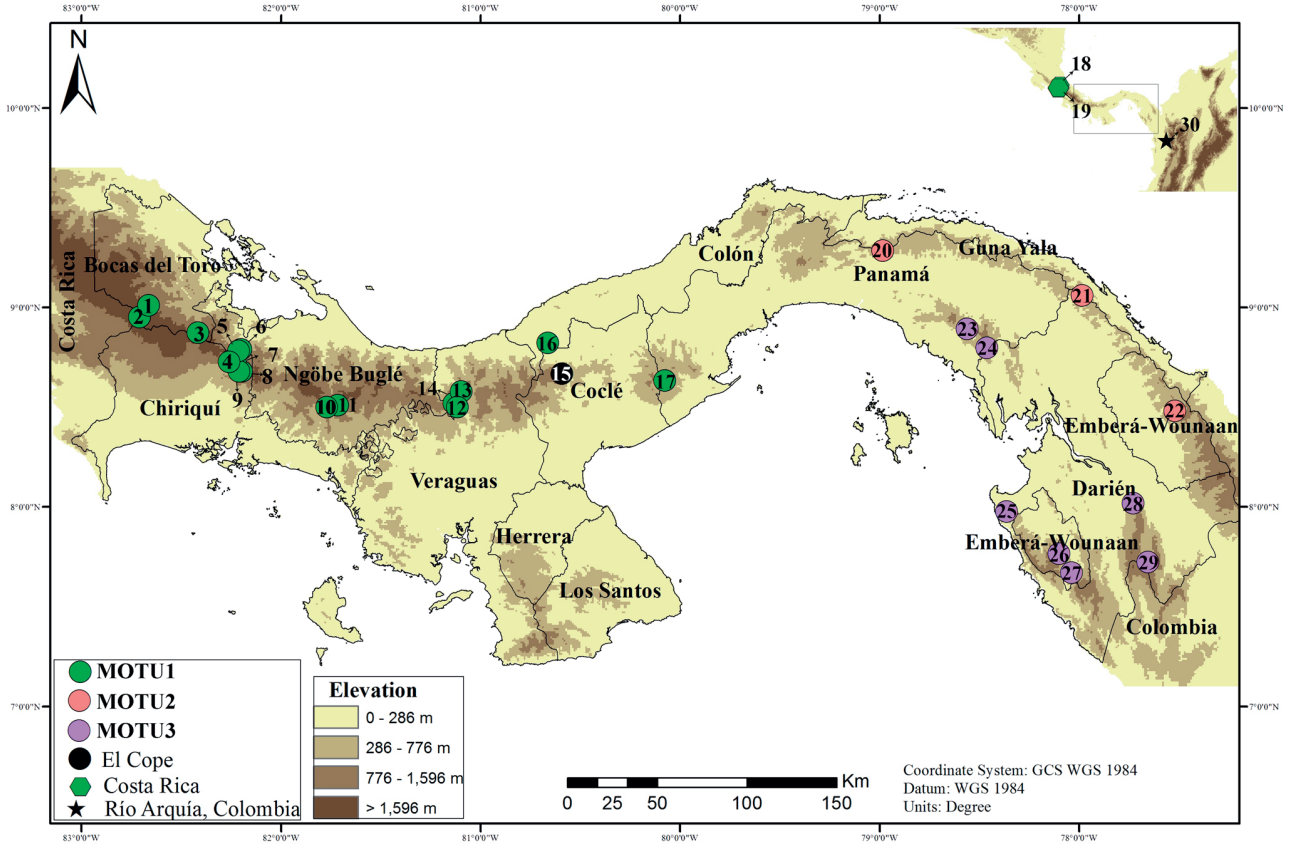

Figure 1. Localities of specimens of the *Pristimantis caryophyllaceus* complex mentioned in this study (Panama main map), lower Central America and northern Colombia (inset). Green colour represents MOTU1, pink MOTU2, and purple MOTU3. The black circle indicates El Copé, and the black star (inset map) refers to one locality in Colombia. One symbol may consolidate several localities close to each other; see text for details. (1) Río Clarito; (2) Río Changena; (3) Sendero El Pianista; (4) Fortuna village; (5) Quebrada Arena; (6) Willie Mazú; (7) Sendero los Tucanes, BP Palo Seco; (8) RF Fortuna; (9) Lost and Found; (10) western slope of Cerro Santiago, La Nevera; (11) Llano Tugrí; (12) Brazo de Mulaba; (13) Cerro Negro; (14) Cerro Mariposa; (15) El Copé; (16) Quebrada Valle Grande, Donoso; (17) Altos del María; (18) Tapanti bridge, Costa Rica; (19) Río Gacho, Costa Rica; (20) Río Terable and Burbayar; (21) Nurra; (22) Río Tuquesa; (23) Ambroya, Majé; (24) Chucantí, Majé; (25) Cerro Sapo; (26) Cerro Garra Garra, Jingurudó; (27) Cerro Bailarín, Jingurudó; (28) Pirre; (29) Cana field station; (30) Río Arquía, Colombia.

ern Panama, and the Tabasará and Talamanca mountain ranges in western Panama (Fig. 1). We evaluated the abundance of members of the *Pristimantis caryophyllaceus* complex by opportunistic search for frogs in the leaf litter and undergrowth along trails. Search transect lengths were calculated with the tracking function of a Garmin GPSmap 60CSx. All georeferences were recorded in the WGS 1984 datum format. Maps and transects were created and calculated using ArcGIS 10 (ESRI 2009). Collected specimens were euthanised with T61, fixed with 5 ml of formalin (10%) in 1 l of ethanol (94%), and subsequently stored in ethanol (70%). All figures incorporated herein have been digitally improved and combined using Adobe Photoshop CS3. For candidate species and their delimitation, we follow the integrative concept of Vieites et al. (2009).

Molecular laboratory and phylogenetic inferences

MtDNA was extracted from fresh muscle or liver tissue. The mitochondrial 16S mtDNA was amplified using a Mastercycler pro S (Eppendorf, Hamburg, Germany) by performing an initial denaturation for 1 min at 94°C followed by 35 steps with denaturation for 9 s at 94°C, annealing for 27 s at 45°C, and elongation for 1.5 min at 72°C. Final elongation proceeded for 7 min at 94°C. For the nuclear RAG1 (Recombination Activating Gene 1) we used 1 cycle: 2 min at 96°C; 45 cycles: 20 s at 95°C, 25 s at 52°C, 2 min at 72°C; 1 cycle: 7 min at 72°C. The reaction mix consisted of 1 µl mtDNA template, 2.5 µl Reaction Buffer x10 (PeqGold), 4 µl 2.5 mM dNTPs, 0.4 µl (containing 2.5 units) Taq Polymerase (PeqLab), 14.1 µl H_2O, 1 µl 25 mM $MgCl_2$, and for 16S 1 µl per primer (containing 10 pmol, forward: L2510, 5'-CGCCTGTTTATCAAAAACAT-3'; reverse: H3056, 5'-CCGGTCTGAACTCAGATCACGT-3'; eurofins MWG Operon), and for RAG1 3 µl per primer (forward: R182, 5'- GCCATAACTGCTGGAGCATYAT -3'; reverse: R270, 5'- AGYAGATGTTGCCTGGGTCTTC -3'; eurofins MWG Operon, Heinicke et al. 2007). The COI gene was sequenced at the Southern China DNA Barcoding Center. In total we could sequence eleven samples (eight 16S, seven COI, and nine RAG1). We compared the mtDNA data of our specimens with that published for thirteen specimens in GenBank (thirteen sequences for 16S & COI and four for RAG1). The sequences were aligned with CLUSTAL W and edited visually using Geneious version 6.1 (Biomatters Inc., available online from http://www.geneious.com/). A list of specimens included in our genetic analysis with corresponding GenBank accession numbers is presented in Supplementary Table S5. *P. cerasinus* and *P. cruentus* were used as outgroups. The final alignment of the 16S mtDNA comprised 24 sequences of 473 bp in length, of which 110 sites were variable and 82 were parsimony-informative. The final alignment of the COI gene comprised 19 sequences consisting of 559 bp, of which 189 sites were variable and 158 sites were parsimony-informative. For 18 specimens, we analysed sequences of both genes, allowing us to combine COI and 16S genes consisting of 1032 bp, of which 292 were found to be variable and 233 sites parsimony-informative. Only ten samples of combined mitochondrial genes and the nuclear RAG1 gene were obtained (excluding outgroups), consisting of 1653 bp, of which 1523 sites were variable and 1461 were parsimony-informative. Using MEGA6 (Tamura et al. 2011), we computed uncorrected pairwise genetic distances for COI and 16S both separately and combined. For each gene and for the combined-gene data set, we conducted Maximum Likelihood (ML) analyses, using the Tamura-3-Parameter, with 1,000 bootstrap replicates. Prior to model-based phylogenetic inferences, JModeltest 0.1.1 (Posada 2008) was used under the corrected Akaike Information Criterion (AICc) to select the substitution model for the Bayesian analysis. We ran a Bayesian phylogenetic analysis in MrBayes 3.1.2 (Huelsenbeck & Ronquist 2001) for 20,000,000 generations with four default chains, sampling every 100th generation and subsequently discarding 5% as burn-in. To test species delimitation in the case of *P. educatoris – P. caryophyllaceus*, we applied two different methods. First, we conducted a statistical parsimony network analysis with gaps considered as a fifth character state (only for COI) in TCS v1.21 (Clement et al. 2000). In order to connect all haplotypes we set the connection limit to 15 steps. Second, we used the Automatic Barcode Gap Discovery (ABGD) algorithm (Puillandre et al. 2011) under the following settings: steps = 20, distance = Kimura 2-parameter model with a transversion/transition ratio of 2.0, and the setting for the minimum relative gap width (X) varied at values between 0 and 1.5. The MOTU's phylogenetic relationships and divergence times were estimated for the mtDNAs 16S and COI, and the nDNA RAG1 (10 individuals and 1,699 bp), using the program BEAST 1.5.4 (Drummond & Rambaut 2007), with a relaxed clock, allowing substitution rates to vary according to an uncorrelated log-normal distribution, assuming a Yule tree prior (Drummond et al. 2006). The prior distributions of substitution parameters were set as default, and to calibrate the root and one node age, respectively, we used an age of approximately 32 million years (Mya) with a standard deviation of seven million years for the splitting of the related species *P. cerasinus* and *P. cruentus* from *P. caryophyllaceus*, and together with the maximum and minimum estimated crown ages (10.4–14.4 Mya) for the *P. caryophyllaceus* clade obtained by Pinto-Sánchez et al. (2012). Every MOTU was treated as a monophyletic group. Parameters were estimated using 100 million generations with a burn-in of 10 million generations, and trees were sampled at every 10,000th generation. Results were visualized and compared using Tracer 1.5 (Rambaut & Drummond 2009), and summary trees were generated using TreeAnnotator 1.5.4.

Morphometrics

Morphological nomenclature, measurements and diagnosis follow Duellman & Lehr (2009) and Köhler (2011). All measurements were taken with digital callipers and rounded to the nearest 0.01 mm. Measurements are giv-

en as mean ± standard deviation and range in parenthesis (Supplementary Tab. S1). Specimens were deposited in the Museo Herpetológico de Chiriquí (MHCH) at the Universidad Autónoma de Chiriquí, Panama, and the Senckenberg Research Institute and Nature Museum (SMF), Frankfurt, Germany. Morphological data of similar *Pristimantis* species used for comparisons were taken from the respective original descriptions.

The following morphometric measurements were taken (with abbreviations): snout–vent length (SVL); head length (HL), diagonally from angle of jaw to tip of snout; head width (HW), between angles of jaws; interorbital distance (IOD); eye length (EL), from anterior to posterior edge of externally accessible eye; eye to nostril distance (END), from anterior edge of eye to posterior corner of nostril; internarial distance (IND), between centres of nostrils; forearm length (FAL), from proximal edge of palmar tubercle to outer edge of flexed elbow; hand length (HAL), from proximal edge of palmar tubercle to tip of third finger; tibia length (TL), as the distance from the knee to the distal end of the tibia; foot length (FL), from proximal edge of outer metatarsal tubercle to tip of fourth toe; width of third finger (3FW), at penultimate phalanx just anterior to disk; width of disk of third finger (3FD), at greatest width; width of fourth toe (4TW), at penultimate phalanx just anterior to the disk; width of disk of fourth toe (4TD), at greatest width; and tympanum diameter (TYMP), measured horizontally, supposing an approximately circular tympanum. We determined the sexes of adults by differences in SVL (males smaller than females), the presence of vocal slits in males, and the presence of eggs in females. Specimens with a SVL < 15 mm were classified as juveniles and excluded from the morphological analyses.

We sorted genetic lineages into Molecular Operational Taxonomic Units (MOTUs) to investigate morphological differences among these MOTUs. To test such differences between taxa currently assigned to *P. caryophyllaceus* and *P. educatoris,* we provisionally classified specimens from west of the Fortuna depression as members of the former species, whereas specimens from east of Fortuna were allocated to the latter species. We furthermore used the condition of the subarticular tubercles according to Ryan et al. (2010) as a character to distinguish between both taxa. The statistical analyses were performed using SPSS 17.0.

Bioacoustics

Advertisement calls were recorded using a Marantz Professional (PMD 620) or a Panasonic RR-XS410 digital recorder with a Sennheiser ME 66 shotgun microphone capsule with a Sennheiser K6 powering module that were set up at distances of 0.5 to 1.5 m from the calling male. Ambient temperature and humidity were measured using an Oakton digital thermo-hygrometer. Males were recorded at a sampling rate of 44 kHz and 16-bit resolution. Recordings were made in uncompressed PCM format and saved as wav-files. The spectral and/or temporal parameters were analysed and the power spectra calculated in Raven Pro 1.4 (Window: Blackman, DFT: 2048 samples, 3 dB filter bandwidth: 158 Hz; Grid spacing 21.5 Hz; overlap 70.1%; Charif et al. 2004). Lowest and highest frequencies were measured 20 db below peak frequency. Terminology used in the advertisement call description follows Duellman & Trueb (1994). To calculate call rates, we divided the average call duration by 60 (sec.) plus the average of call intervals.

Colour variation

Generalized colouration summaries were derived directly from live specimens or indirectly from photos of live specimens. Within the standardized colour descriptions of selected individuals, the capitalized colours and colour codes (the latter in parentheses) are those of Smithe (1975–1981).

Results

Based on the lineages resulting from our phylogenetic analysis (see section on molecular phylogenetics below), we assigned each specimen to one of three MOTUs. The MOTUs were largely consistent with a geographical pattern and defined as follows (Fig. 1): MOTU1 contains specimens from western Panama, MOTU2 from eastern Atlantic Panama (Daríen and San Blas mountain ranges), and MOTU3 from eastern Pacific Panama (Jingurudó, Majé, Pirre and Sapo mountain ranges). Taking into account the congruence between the phylogenetic results and the biogeographical pattern, we assigned 78 measured specimens to their respective MOTUs, with 53 to MOTU1, 18 to MOTU2, and seven to MOTU3. In the following, we present the results of our analyses of molecular genetics, morphometrics, colour variation, natural history, geographic distribution, and vocalisation of the *Pristimantis caryophyllaceus* species complex.

Molecular genetics

MOTUs based on mitochondrial data usually contained samples only from one biogeographical region, except the samples from El Copé, which are represented in all three MOTUs by at least one sample. No nuclear genetic data were available for El Copé samples to elucidate their congruence to mitochondrial data, and investigate the potential of introgression among MOTUs at El Copé. The tree topology of the combined mitochondrial genes (Fig. 2) and the COI alone (Supplementary Fig. S1) were basically congruent. The distances between and within MOTUs are shown in Table 1 (see also Supplementary Tabs S2–S4 for genetic distances between MOTUs).

In the parsimony network analysis based on the 16S gene, seven samples formed unconnected haplotype networks, and six did so in the analysis of the COI gene. The samples from El Copé in MOTU1 were connected to the

sample from Donoso (MOTU1) with eight mutational steps between them in the 16S network and four in the COI. The samples from Altos del María, Panama and Río Gacho, Costa Rica, were connected to nine unsampled haplotypes in the 16S network, but were not connected in the COI network; one sample from Tapantí, Costa Rica, was connected to the samples from Río Changena and Río Clarito, Bocas del Toro, with 12 unsampled haplotypes between them (only one of these samples was included for COI). In MOTU2, only the samples from El Copé were grouped in the same haplotype, in both 16S and COI. In MOTU3, the samples from the Majé and Jingurudó mountain ranges (16S and COI), as well as those from the Cana field station (COI) were connected. Our ABGD analysis generated five groups for 16S with a divergence threshold of 0.022 with a relative width of the barcoding gap of 0.05 in the X-value. For COI, it produced eight groups, assuming an a priori intraspecific divergence threshold of 0.068 with a relative gap width of 0.05 (X-value), whereas ten groups resulted when both genes were combined (threshold of 0.048). Our three analyses (16S, COI, and both genes combined) lumped all samples in one unit, with a priori intraspecific divergences of 0.030, 0.088, and 0.062, respectively. With ABGD, all samples from MOTU2 and almost all from MOTU1 for the COI and 16S sequences (Supplementary Figs S1–S2) were grouped in their corresponding geographic MOTU. The 16S ABGD assigned all samples of MOTU1 to one cluster, but also included samples from Majé that were placed in MOTU3 according to our phylogenetic analyses. One sample from El Copé (USNM 572338) did not nest within any cluster in the 16S analysis, but took a place within MOTU3 when using COI and both genes combined.

According to our divergence time estimates, the MOTUs started to diverge from other species of the subgenus *Hypodictyon* Cope, 1885 (sensu Hedges et al. 2008), which were present in Central America in the Oligocene 23.16 Mya (with a 95% credibility interval, CI, of 17.33–29.46 Ma). The crown age of the MOTUs dates to 13.27 Mya (CI: 11.38–14.39 Mya) during the Miocene, when MOTU1 and MOTU2 + MOTU3 split; a second break between the ancestors of MOTU2 and MOTU3 occurred 12.19 Mya, followed by several splitting processes within the respective MOTUs between 7.6 and 3.5 Mya. When all genes were used in the phylogenetic analysis, the ML analysis yielded a consensus tree that was topologically congruent with the divergence-time tree. However, in the divergence-time analyses, when each MOTU was treated as a monophyletic group, the Majé samples were nested within MOTU1, showing a divergence-time of 11.12 Mya. This is not supported (p = 0.66, see Supplementary Fig. S4), however, although when the MOTUs were not supposed to be monophyletic, the posterior probability for the divergence-time analysis was not supported either (p = 0.54, Fig. 3 and Supplementary Fig. S3).

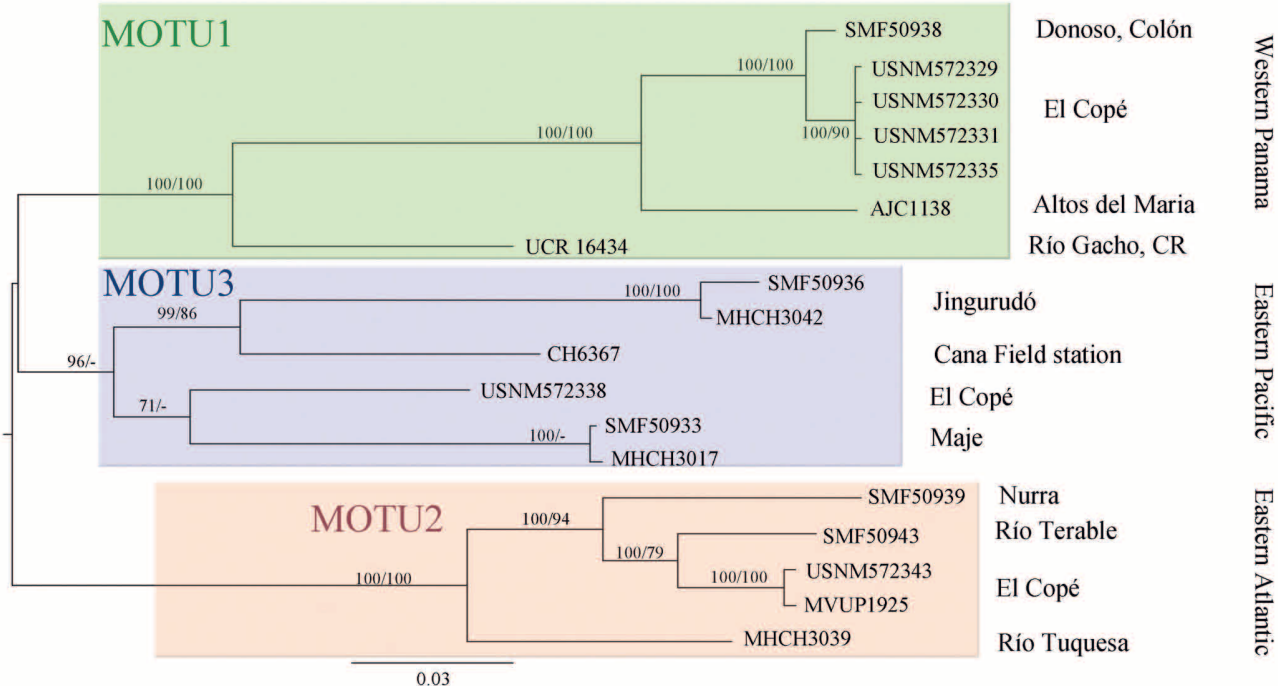

Figure 2. Maximum likelihood tree of the combined COI and 16S mtDNA sequences of the *Pristimantis caryophyllaceus* complex. Specimen labels refer to collection or museum numbers. Colour shadings of MOTUs correspond to those in Figure 1. Scale bar refers to number of substitutions per site. Maximum likelihood bootstrap values are shown above branches, and Bayesian posterior probabilities (multiplied by 100) below slash. Tree, midpoint root tree.

Table 1. Tamura 3-parameter distances among the *Pristimantis caryophyllaceus* (including "*P. educatoris*") specimens used in this study. MOTU: MOTU1 contains specimens from western Panama, MOTU2 from eastern Atlantic Panama (Daríen and San Blas mountain ranges), and MOTU3 from eastern Pacific Panama (Jingurudó, Majé, Pirre and Sapo mountain ranges).

Genes	Average genetic distance	Distance within MOTUs			Distance between MOTUs		
		MOTU1	MOTU2	MOTU3	MOTU1-MOTU2	MOTU1-MOTU3	MOTU2-MOTU3
16S	6.5	4.02	1.49	6.1	7.15	7.53	8.9
COI	14.98	6.86	7.23	9.91	19.96	18.13	15.75
16S + COI	12.43	5.4	5.53	9.12	16.05	14.8	13.76

Morphometrics

In Supplementary Table S1, we present the morphometric variables used to evaluate the differences between lineages within the *Pristimantis caryophyllaceus* complex. Our morphological analysis revealed differences between the three MOTUs (Fig. 4). A Discriminant Function Analysis (DFA) classified 83.3 % of the specimens according to our a priori groupings (94.3% MOTU1; 71.4% MOTU2; 55.6% MOTU3). The principal morphological variables contributing to the grouping were 1) TYMP/SVL, 2) 4TD/4TW, 3) IOD, 4) 3FD; the first function is: DS = 0.63 * TYMP/SVL + 0.44 × 4TD/4TW + 1.23 × IOD + -0.88 × 3FD; and the second function is DS = -0.55 × TYMP/SVL + 0.123 × 4TD/4TW + 0.17 × IOD + 0.66 × 3FD. The specimens included in MOTU3 are usually larger than those from MOTU2 and MOTU1, respectively. Likewise, MOTU2 and MOTU3 seem to be more similar to each other (MOTU2 → MOTU3: 28.6%) than either of them is to MOTU1 (3.8% and 1.9%, respectively; see Figs 4 + 5).

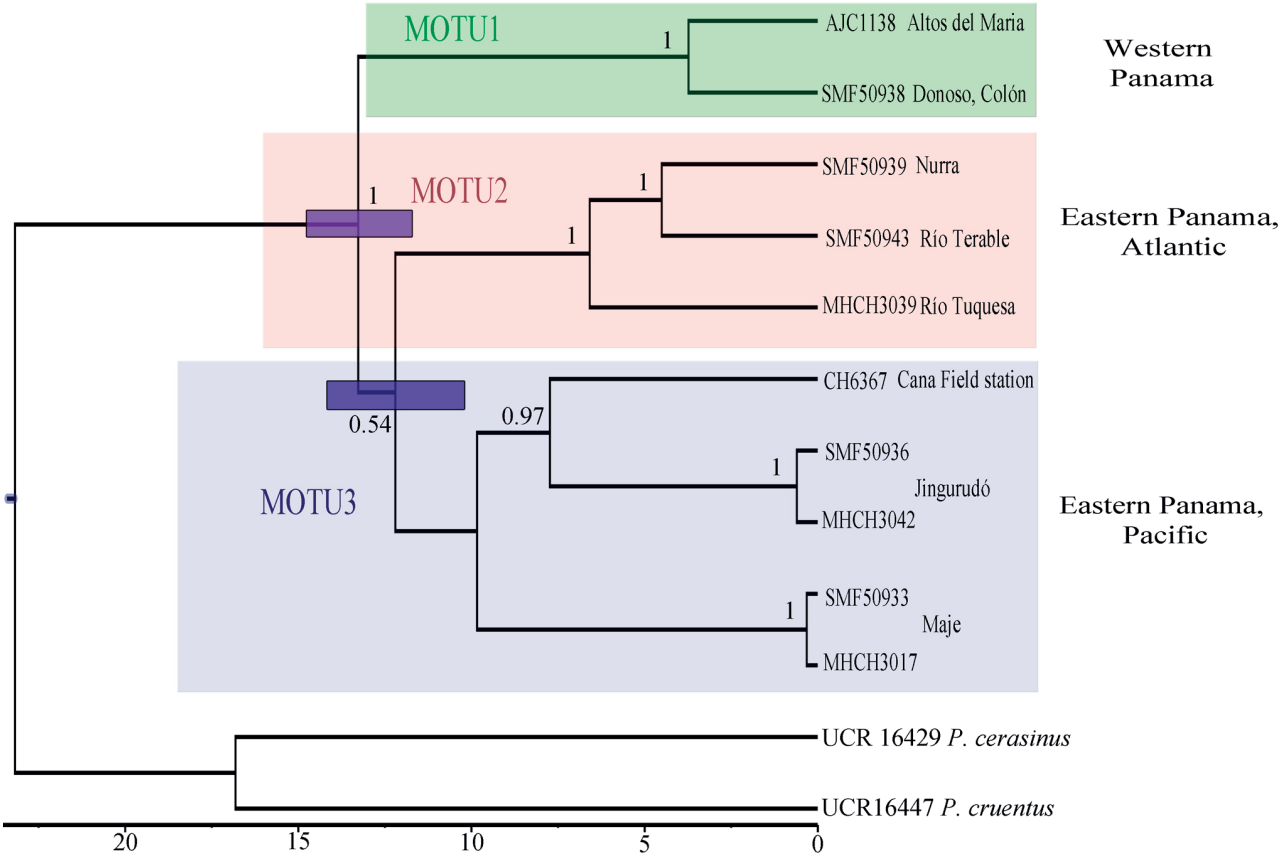

Figure 3. Timetree of *Pristimantis caryophyllaceus* based on RAG1, 16S and COI genes, with *P. cerasinus* and *P. cruentus* as outgroups. Scale along the bottom indicates time in millions of years (Mya). Colour of shading reflects MOTU designations (for species at tips), as in Figs 1 and 2. Blue horizontal bars indicate 95% credibility intervals for the divergence time of the MOTUs. Numbers on nodes indicate estimated posterior probabilities for the presence of the corresponding clade according to BEAST (see text for details).

Our analysis of differences between specimens from west of Fortuna, alias *Pristimantis caryophyllaceus*, and east of Fortuna, alias *P. educatoris* sensu Ryan et al. (2010), showed differences between each other, both according to geography (MANOVA, Pillai's trace = 0.66, $F_{12, 44}$ = 7.20, P < 0.05) and based on the condition of subarticular tubercles (MANOVA, Pillai's trace = 0.34, $F_{11, 45}$ = 2.13, P = 0.04). The DFA classified specimens on the basis of geography from western and eastern Panama correctly, with 98.4% probability, into their respective groups (DFA = 1.12 × 3FD/3FW + 0.67 × IOD/HW + 1.37 × EL + -1.68 × 3FD + 0.45 × 4TD/4TW), and when using the condition of subarticular tubercles, the DFA classified the two MOTUs with 70.5% probability into their original groups (DFA = 1.31 × EL + 0.70 × 4TD/4TW + -0.98 × SVL).

Colour variation

Pristimantis caryophyllaceus is one of the most polychromatic species in its genus. The general dorsal colouration varied from yellow to reddish with various brownish tonalities, with or without black chevron marks on the dorsum, and sometimes with sulphur-yellow spots on

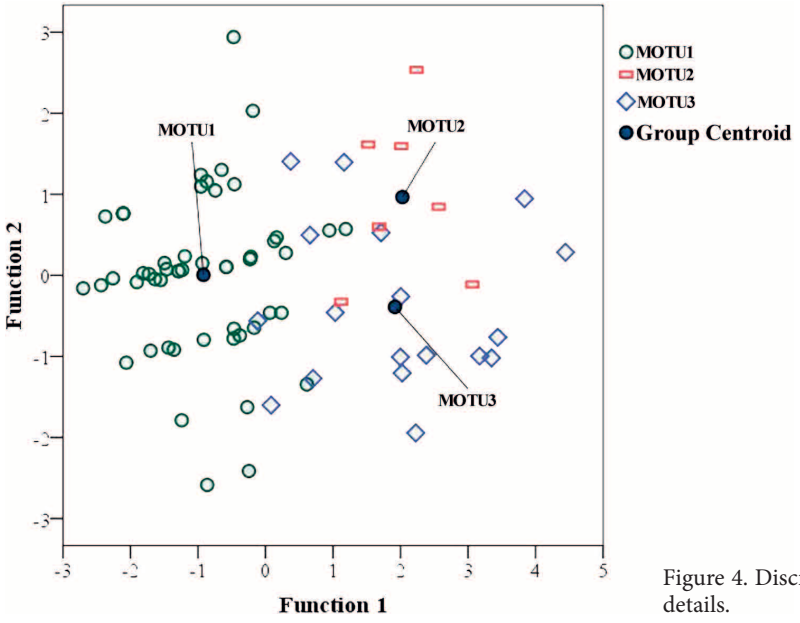

Figure 4. Discriminant function analysis of MOTUs; see text for details.

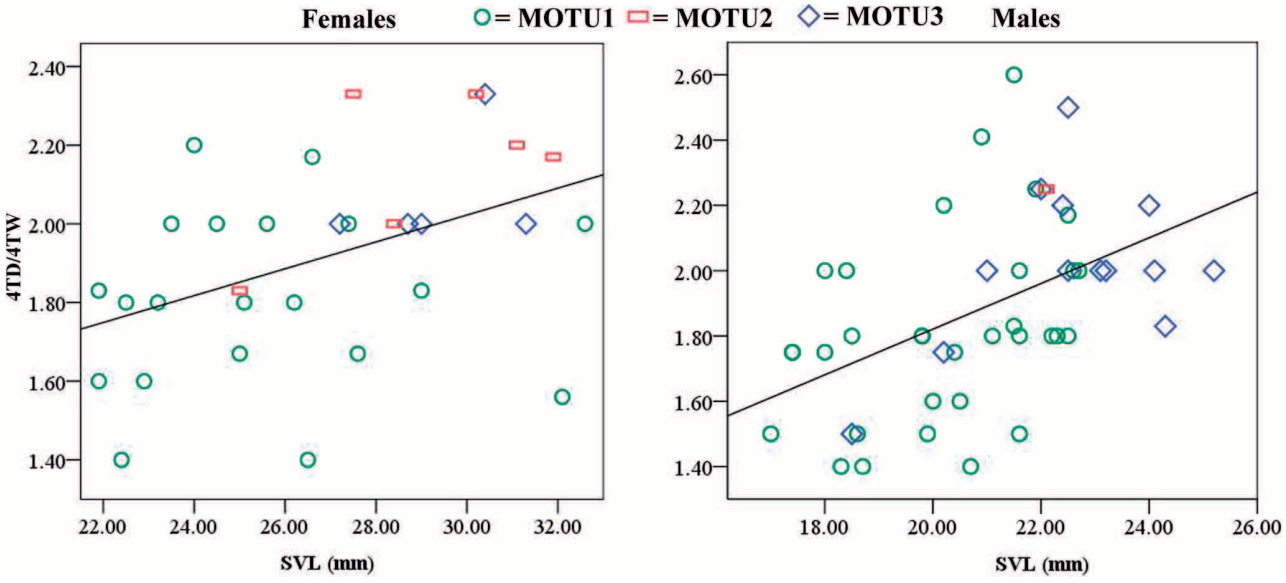

Figure 5. Relation between SVL and the expanded disk condition on the fourth toe of *Pristimantis caryophyllaceus* complex-MOTUs. Females (r^2 = 0.20; P = 0.014) and males (r^2 = 0.26; P = 0.005).

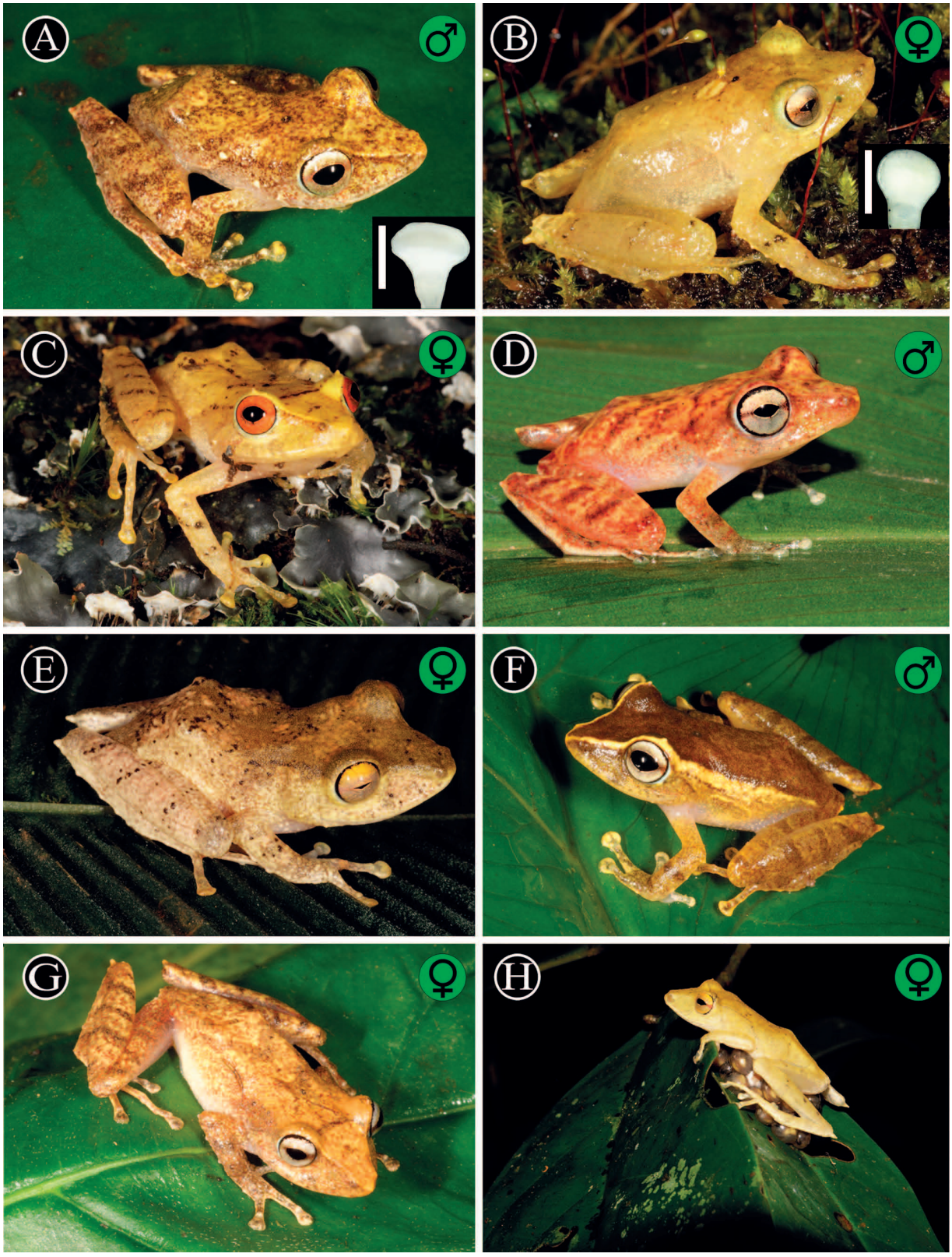

Figure 6. Colour variation in the *Pristimantis caryophyllaceus* complex. (A) Río Clarito (SMF 97037); (B) Río Changena (SMF 97035); (C) Río Changena (SMF 97034); (D) Valle grande, Donoso (SMF 50938); (E) Willy Mazú (SMF 97033); (F) La Nevera (SMF 97031); (G) Llano Tugrí (SMF 97030); (H) female during maternal care, Alto de Piedra. Colours of circles correspond to the MOTUs in Figure 1, Sex: ♀ = female, ♂ = male.

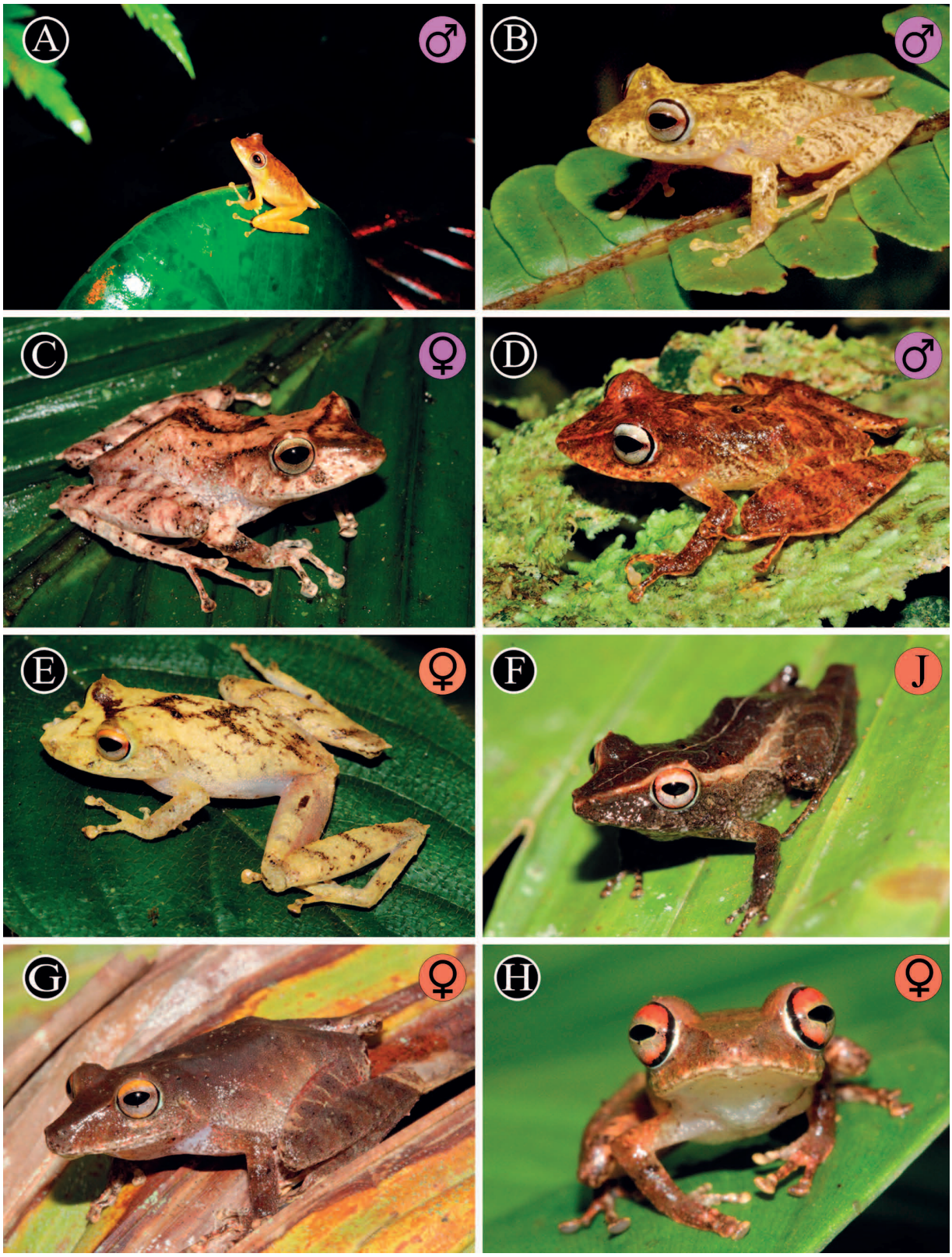

Figure 7. Colour variation in the *Pristimantis caryophyllaceus* complex. (A) Cerro Sapo (MHCH 3022, recorded); (B) Cerro Sapo (MHCH 3021); (C) Cerro Garra Garra, Jingurudó (MHCH 3042); (D) Cerro Bailarín, Jingurudó (SMF 50936); (E) Río Tuquesa (MHCH 3039); (F) Nurra (MHCH 3037); (G) Nurra (SMF 50939); (H) Nurra (SMF 50940). Colours of the right corner circles correspond to the MOTUs in Figure 1. Sex: ♀ = female, ♂ = male, J = juvenile.

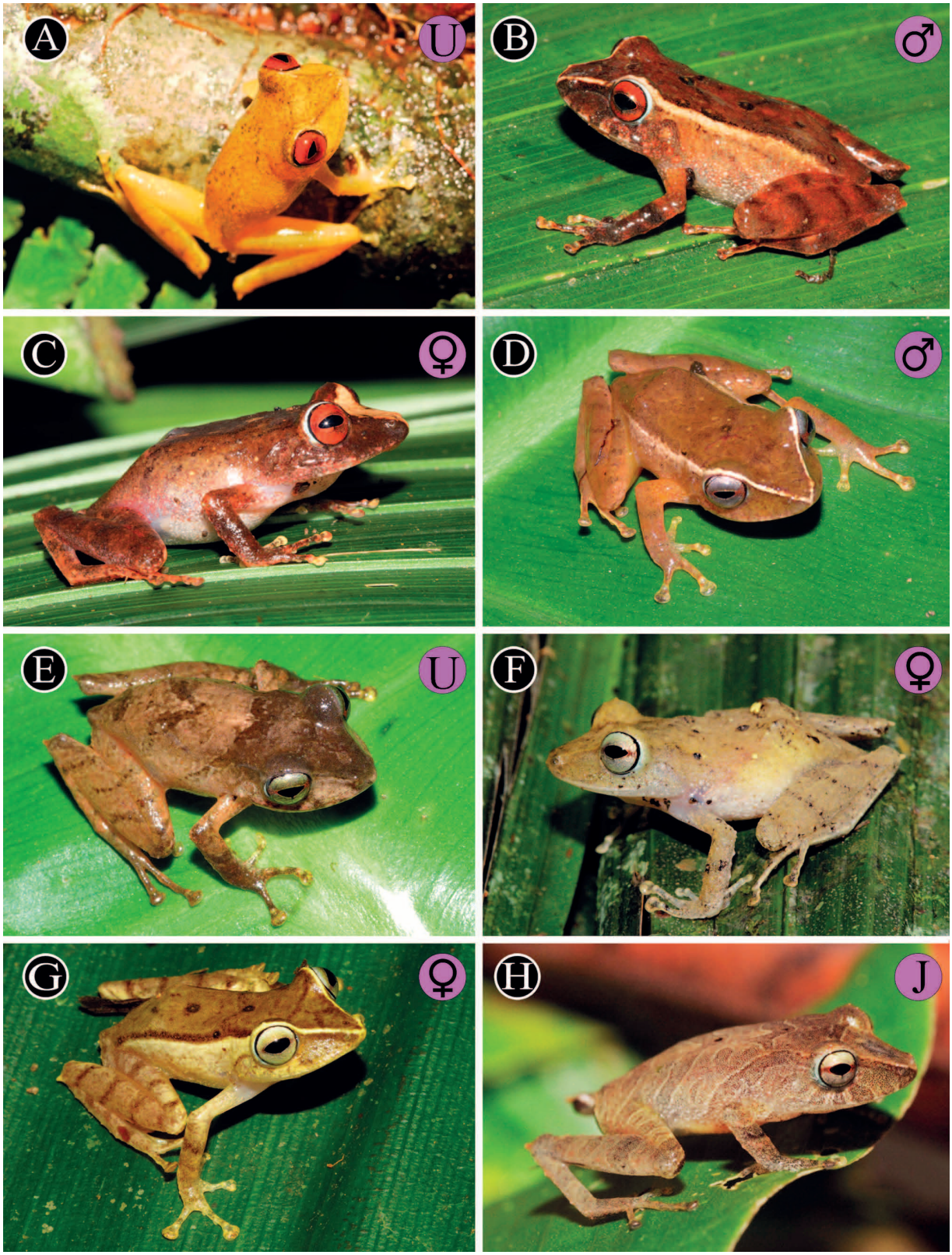

Figure 8. Colour variation in the *Pristimantis caryophyllaceus* complex. (A) Ambroya, Majé; (B) Chucanti, Majé (SMF 50945); (C) Chucanti, Majé (MHCH 3043); (D) Chucanti, Majé; (E) Chucanti, Majé; (F) Pirre (SMF 50946); (G) Pirre (MHCH 3045); (H) Cana Field station (MHCH 3019). Colours of right corner circles correspond to the MOTUs in Figure 1. Sex: ♀ = female, ♂ = male, J = juvenile, U = unidentified.

Table 2. Spectral and temporal parameters of the advertisement call of *Pristimantis caryophyllaceus*. The specimen MHCH 3022 was the only one collected, recordings 1–3 correspond to males that were not captured (see Vocalisation section for explanation). Averages for the parameters are given in the Resume column.

Variables	Males				Resume
	MHCH 3022	Recording 1	Recording 2	Recording 3	
Length recording (min)	00:20:10	00:20:10	00:11:09	00:08:26	00:59:55
Date	05-Dec-12	05-Dec-12	06-Dec-12	26-Aug-13	
Time	19:12	19:12	17:40	19:18	
SVL (mm)	22.50				
Temperature (°C)	19.4	21.6	21.6	22	21.15
Humidity (%)	83	63	63		52.25
Number of calls	1	2	3	1	7
Number of call intervals	n/a	1	2	n/a	3
Number of pulses	6	14	23	8	51
Number of pulse intervals	5	12	20	7	44
Call duration (s)	0.04	0.04	0.04	0.05	0.040±0.004 (0.035–0.046)
Call interval (s)		181.87	135.55		151±26.74 (135.45–181.87)
Call rate (call/min)	0.44		0.33		0.39±0.08 (0.33–0.44)
Pulses/call (s)	6.00	7.00	7.67	8.00	7.28±0.76 (6–8)
Pulses/duration (s)	0.003	0.003	0.004	0.003	3.34x10-3±0.7x10-3 (2.0x10-3–4.0x10-3)
Pulses/interval (s)	0.003	0.003	0.002	0.003	2.41x10-3±0.75x10-3 (1.0x10-3–4.0x10-3)
Lowest Freq (kHz)	2.48	2.30	2.24	2.41	2.32±0.11 (2.18–2.48)
Highest Freq (kHz)	3.25	3.69	3.16	3.31	3.34±0.25 (3.13–3.77)
Delta Freq (kHz)	0.76	1.38	0.92	0.90	1.03±0.26 (0.76–1.4)
Energy (dB)	85.30	82.90	88.13	107.60	89.01±9.52 (80.3–107.60)
Max. Freq (kHz)	2.76	3.01	2.56	2.80	2.75±0.23 (2.43–3.17)

the dorsum and/or limbs (Figs 6–8). Groin and posterior thigh varied from not contrasting in colour to yellow or red. *Pristimantis caryophyllaceus* also had a highly variable eye colouration, which appears not to be correlated to the dorsal colour pattern (Figs 6–8), with specimens with a red iris showing reddish (Figs 7H, 8C), yellowish (Figs 6C. 8A), uniform or striped (8B) dorsal colour patterns, as did specimens with a pale iris colouration (Figs 6–8); specimens from the same population were found to have a red, grey or cream-coloured iris (Fig. 6). A detailed colour description of specimens in life is included in Supplementary Text S6.

Vocalisation

During our trip to Cerro Sapo, we recorded four males of MOTU3, of which only one was subsequently collected (MHCH 3022, Fig. 8A). From one recording, calls of two different males could be analysed. One male was calling closer, about 0.4 m from the microphone, and the other one called from a distance of about 1.0 m. Thus, the call of the first male (MHCH 3022) appeared louder in the Raven 4.1 waveform and allowed to easily differentiate between both individuals. In the first recording (Recording1 in Tab. 2), both males were calling from a bush 1.0 m above the ground and could be observed during the recording. Simultaneously, a third male was observed, calling from a distance of approximately 2 m, but was not recorded. The next day (06/12/12, see Tab. 2), we recorded a fourth male (at 7.97692° N, 78.35969° W; 966 m a.s.l.; not captured) calling from a bush 1.5 m above the ground (Recording 2 in Tab. 2). During a second trip to Cerro Sapo, we recorded another male (at 7.97944° N, 78.35507; 834 m a.s.l.) calling from an epiphytic orchid about 0.7 m above the ground (Recording 3 in Tab. 2).

Pristimantis caryophyllaceus from MOTU3 were active at night, and males were calling sporadically throughout the night. No calls from specimens were recorded from locations other than Cerro Sapo. However, A.B. has heard and seen (but not recorded) males calling at La Nevera and Reserva Forestal La Fortuna (western Panama).

The vocalisation produced by *Pristimantis caryophyllaceus* from MOTU3 consists of a single, pulsed note that is reminiscent of a sound like "chack" and emitted at 2.75 ± 0.25 kHz (2.43–3.17; Fig. 9, Tab. 2); with a note duration of $38^{-3} \pm 3.0^{-3}$ s (35^{-3}–43^{-3}) and repeated sporadically every 151 ± 26.74 s (135.45–181.87). Every note has from six to eight pulses. The call rate is 0.39 calls/min. Although there are no recorded calls to compare the vocalisation of different MOTUs of *P. caryophyllaceus*, the call of western Panamanian specimens is also a "chack" sound that is repeated sporadically and sounded very similar to calls of specimens from eastern Panama.

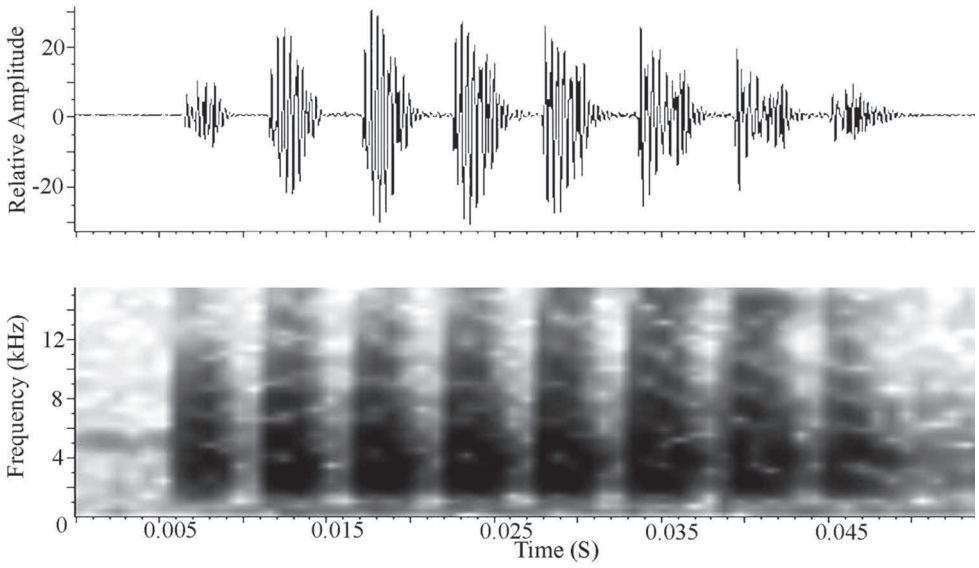

Figure 9. Oscillogram (top) and spectrogram (bottom) of the advertisement call of a *Pristimantis caryophyllaceus*-complex-male, recorded at Cerro Sapo (MHCH 3022).

Natural history notes

Frogs of the *Pristimantis caryophyllaceus* complex are primarily inhabitants of pristine forest, but are also found at the edges of forests. During seven nighttime transect searches in eastern Panama (Jingurudó, Pirre and Sapo mountain ranges), we observed 46 individuals (see Supplementary Tab. S6). The relative abundance was 2.6 indv./ 100 m trail transect; most specimens were found at heights between 0.2–2.5 m above the ground perched on bush leaves and the bark of trees. These frogs are direct-development breeders (Savage 2002), and reproduction occurs during the rainy season. Their reproductive behaviour and, especially, the maternal care have been described in detail by Myers (1969) and Ryan et al. (2010) (see also Fig. 6H).

These frogs feed on a variety of invertebrates: collembolans, cicadas, terrestrial planarians, isopods, arachnids, larvae (caterpillars, dipterans), wasps, and crickets (Batista 2009, Lieberman 1986). In one population analysed from the Burbayar Field Station in the San Blas mountain range (MOTU2; see Supplementary Tab. S5), the stomach contents of seven individuals comprised 21 prey items of 10 different taxonomic groups (see above); with 2.56 $\pm$ 3.10 mm^3 in average volume of prey. The niche breadth for this population was 6.37 (Batista 2009), whereby a value near one suggests that a species would prey exclusively on one prey category, and a value higher than one indicates that a species exploits a greater variety of prey categories (Pianka 1986, Vitt & Caldwell 1994). Thus, this species can be considered a dietary generalist. At La Nevera (MOTU1), another population of the *P. caryophyllaceus* complex was analysed (Batista 2009), but few specimens were caught, and the three stomachs analysed yielded only three prey items (one each): two crickets and one arachnid, with an average volume of 1.77 $\pm$ 1.47 mm^3.

Discussion

Our results demonstrate a high level of genetic diversity in the *Pristimantis caryophyllaceus* complex, comprising three main lineages within its currently known distribution (this study, Crawford et al. 2010, Pinto-Sánchez et al. 2012). Such a scenario has been found before, i.e., in *P. ridens* in Central America (Wang et al. 2008). The three main lineages, classified here as MOTUs, appear to be very old with an estimated crown age between 10.4–14.4 million years ago (Pinto-Sánchez et al. 2012). Due to the great genetic distances between the individual MOTUs, they could be considered three Unconfirmed Candidate Species (UCS) (Vieites et al. 2009, Crawford et al. 2010) that are statistically supported by some morphometric differences (e.g., TYMP/SVL, 4TD/4TW), which would normally support granting them specific status. However, considering the many shared traits among these MOTUs, such as the intricate results obtained from the haplotype network, the lumping of all samples in one species with low values of prior genetic distance (ABGD analyses), the high morphological variation exhibited within the MOTUs compared to that between the MOTUs, the difficulty to differentiate their phenotypes in the field, and their similarities in ecology and behaviour, these MOTUs may just as well be treated as Deep Conspecific Lineages (DCL: Vieites et al. 2009, Padial et al. 2010) of one single species with incomplete lineage sorting among them. The recognition of these MOTUs as separate species would require testing for possible reproductive, genetic, and ecological incompatibilities

in their zones of contact and/or evaluating whether these MOTUs behave/evolve as independent entities.

The ABGD has grouped successfully almost all samples of MOTU1 and MOTU2 for both mitochondrial genes. The most incongruent result obtained in the species delimitation test (ABGD) was the placement of the samples from the Majé mountain range (MOTU3) with the samples from western Panama (MOTU1) in the same group (Supplementary Fig. S2). The over-splitting detected by the ABGD analysis in MOTU3 (Supplementary Figs S1–S2) is likely due to the great genetic distances found within that group, as reflecting the inclusion of specimens from three different isolated regions (Majé mountain range, Jingurudó-Sapo mountains, and Pirre lowlands). In our analyses, the ABGD lumped all MOTUs with a low prior intraspecific divergence (3.0% for 16S, 8.8% for COI, and 6.2% both genes combined), compared to the maximum values of the a priori threshold for conspecific divergence that yielded a primary species hypothesis in the closely related *Pristimantis museosus* (10.0% for 16S, 15.0% for COI and when both genes combined; Crawford et al. 2013).

Earlier studies (Ryan et al. 2010) and our genetic analysis could support splitting the *Pristimantis caryophyllaceus* complex into *P. caryophyllaceus* and *P. educatoris*, or even into three species according to the MOTUs recovered in this study. We also detected morphological, yet non-significant, variation among MOTUs that should not be disregarded until larger samples can be tested to evaluate a potential clinal variation that forms a continuum with the variability detected within the MOTUs (Mallet 2008), corresponding to interbreeding between the MOTUs (e.g., at El Cope), or corresponds to a geographical pattern. For example, the specimens from Río Changena and Río Clarito (MOTU1) share the same haplotype, but the Río Clarito (SMF 97037) frogs have more widely expanded disks than the ones from Río Changena (SMF 97035; Figs 6A–B). Likewise, specimens from the same population in eastern Panama may or may not have expanded disk pads or disk covers. Also, the relation of Toe V and Toe I to the distal subarticular tubercle of Toe IV and Toe II, respectively, is highly variable. According to Crawford et al. (2010), one can find both or even all three lineages in sympatry at El Copé, for which reason there is a potential of substantial interbreeding. We could not detect this to be the case by analysing mitochondrial DNA (O'Donnell & Mock 2012), but this question could be resolved by investigating the nuclear DNA, which is not currently available for all MOTUs. However, the existence of these lineages in sympatry could be an indication of ongoing speciation (Mallet 2008), but this has not been tested yet.

The great colour variation among specimens of the *Pristimantis caryophyllaceus* complex has been pointed out before (Hoffman & Blouin 2000). Glaw & Vences (1997) discussed the eye colouration in *P. caryophyllaceus* on the basis of photographs in Weimer et al. (1993). They also suspected that different taxa might be involved here. The fact of the matter is, however, that the pictures in Weimer et al. (1993) show a red-eyed *P. caryophyllaceus* in Figure 10, but a *P. ridens*-like frog and not a member of the *P. caryophyllaceus* complex in Figure 11. Our comprehensive photographic data and colour descriptions confirm a wide colour variation within and between MOTUs. Specimens with different eye colours from the same populations did not exhibit other morphological differences. Therefore, eye colouration has no diagnostic value, and we are considering specimens with different eye colourations occurring within a MOTU as conspecific and/or members of the same lineage, even though we have no genetic data to corroborate this (no samples with red eyes were sequenced). Ryan et al. (2010) mentioned the presence of yellowish wart-like spots on the dorsum as being characteristic of *Pristimantis educatoris* from eastern Panama. However, we also found specimens with such yellowish marks in extreme western Panama, which otherwise agree with characters of *P. caryophyllaceus* in having rounded pads and disk covers, and low and rounded subarticular tubercles.

The most common polymorphic traits (Ford 1955, Mayr 1963) found in populations of different Terrarana species (Goin 1950, Hoffman & Blouin 2000, Savage & Emerson 1970) relate to characteristics of the dorsal skin texture, colour pattern, and iris colour (Savage 2002). In *P. caryophyllaceus*, polymorphism is most prominent in the dorsal colour pattern, iris colour and digital disk. It seems to be a balanced polymorphism (Ford 1955), inasmuch as it appears to be maintained in the different MOTUs. Colour pattern in Terrarana frogs could be inherited by a simple Mendelian genetic mechanism (Goin 1950, 1960, Summers et al. 2004, O'Neill & Beard 2010), perhaps maintained by the heterogeneity of colour compositions and shapes predominant in the habitat, selective forces exerted by visually guided predators, and fitness-related traits (Hoffman & Blouin 2000, Savage & Emerson 1970, Woolbright & Stewart 2008). At least five different colour patterns were found in a single population of *P. caryophyllaceus* (Figs 8B–E) that were irrespective of sexual affinities, so that sexual dichromatism can be disregarded (see Figs 6–8). Other potential selective agents responsible for maintaining the polymorphism in this species should be targeted in futures studies. Iris colour and the shape of the digital disks are less variable than the dorsal colour pattern, and have widely been used as diagnostic characters to identify anuran species (Glaw & Vences 1997, Lynch & Duellman 1997, Savage 2002, Köhler 2008). Even though intraspecific iris colour variation is known to occur in *Pristimantis* (Lynch & Duellman 1997, Savage 2002, Duellman & Lehr 2009, Fig. 58B), only a few members of this genus have red eyes and none shows the striking variation documented here for *P. caryophyllaceus* (Figs 6–8). Eye colour is usually species-specific and correlated to the dorsal ground colour (Amat et al. 2013), but this is not the case in *P. caryophyllaceus* (see Figs 6–8), where only one species is involved and red eye colour is apparently not linked to the dorsal colour pattern (e.g., Figs 8 A–B).

Most arboreal and semiarboreal Terrarana species have large digital disks, and most ground-dwelling species have small or no digital disks. The function of digital disks is

to facilitate improved climbing in an arboreal environment and would prove beneficial also for semiarboreal activities in Terrarana species (Savage 2002, Hedges et al. 2008). Although the exact function of the digital disks in *P. caryophyllaceus* has not been investigated yet, one possibility could be that the differences in their widths reflect different degrees of arboreality among MOTUs. However, the different degrees of arboreality appear to be not the main reason for this variation, since all specimens were found in the understorey between 0.5 and 2.5 m above the ground on leaves and branches.

The polymorphism found in *P. caryophyllaceus* (sensu lato) appears to be complex and it is not properly reflected by a two-species taxonomy sensu Ryan et al. (2010) or three species as found in this study; i.e., by splitting the species into *P. caryophyllaceus* for western Panama (MOTU1) and two *P. educatoris* taxa for eastern Panama (Caribbean-MOTU2 and Pacific-MOTU3). Based on the molecular information available as of now, all three MOTUs co-occur at El Copé. However, there is no additional evidence for implementing a three-species taxonomy, and sensu Vieites et al. (2009), we would need at least one diagnostic morphological difference, a character trait that is of low intraspecific variability and of high value, to discriminate among taxa (here: MOTUs). The morphological differences between these MOTUs are insufficient to support them as distinct species, however. Furthermore, there are currently no bioacoustic data from El Copé to test for putative interspecific differences.

Ryan et al. (2010) used the SVL to differentiate between *P. caryophyllaceus* and *P. educatoris*. However, rather than a clear difference in SVL, our data suggest a smooth clinal transition of the SVL from east to west (Fig. 5). The condition of a projecting subarticular tubercle, as suggested as a diagnostic character by Ryan et al. (2010), is another trait that is too variable to differentiate between their suggested taxa, as we found both conditions in all three regions. As stated before, the finger and toe disk widths are also variable (see Figs 6A+B). There are two major discrepancies in the species description of *P. educatoris* by Ryan et al. (2010). Firstly, they state that the distribution of *P. educatoris* stretches from Santa Fe eastwards and into Colombia, but according to their Appendix, only specimens from Santa Fe and El Copé were analysed, i.e., two sites in central-western Panama separated by less than 50 km. Hence, clear evidence of an eastern distribution for *P. educatoris* remains wanting. Secondly, they mention a disjunctive population of *P. educatoris* near the Panama border on the Caribbean versant of Costa Rica, but specimens from this site were not included in their analyses and no further information is given on this population. Moreover, this contradicts the biogeographical assumption of the authors' of one species in the west and one in the east with the Fortuna depression as a supposed barrier. Consequently, we can neither finally rule out that *P. educatoris* is a valid species nor can we promote a three-species solution yet, albeit a three-regions separation (MOTU1–3) within the *P. caryophyllaceus-educatoris* populations is evident. Due to the morphological variation within the particular MOTUs and the morphological similarities between the MOTUs, we found no additional evidence to prove the three MOTUs as respective Confirmed Candidate Species (Vieites et al. 2009). Moreover, at this point, we have no evidence for assigning *P. educatoris* to either MOTU2 or MOTU3, and our data do not support the biogeographical concept suggested by Ryan et al. (2010). For now, we suppose to see the three MOTUs within the *P. caryophyllaceus-educatoris*-complex as geographically and genetically distinct lineages in accordance with the definition of a Deep Conspecific Lineage by Vieites et al. (2009) with a small contact zone around El Copé. Consequently, we reject *P. educatoris* as a valid species and place it in the synonymy of *P. caryophyllaceus*.

The phylogenetic history of the MOTUs studied here is linked to the complex biogeography of the Isthmus of Panama and northwestern South America, more precisely of the Choco Block (Duque-Caro 1990 a–b, Coates et al. 2003, 2004), formed by the Majé-Baudó Arc (Majé, Sapo, Jingurudó and Pirre massifs) and the Dabeiba Arc (Darien and San Blas massifs). *Pristimantis caryophyllaceus* has originated in South America (Duellman 2001, Heinicke et al. 2007, Pinto-Sánchez et al. 2012), and its dispersal to Central America is consistent with the recent hypothesis of an earlier formation of the Isthmus of Panama (Farris et al. 2011, Montes et al. 2012), dating well before 3.5 Mya as was previously thought (Coates & Obando 1996, Webb & Rancy 1996, Santos et al. 2009, Weir et al. 2009). The MOTUs show a geographical pattern with almost all MOTUs (except for the El Copé populations) being distributed in different geographic areas (Figs 1–2). According to our results, the split between MOTU1 and MOTU2–MOTU3 (11–14 Mya) supports the proposed connection of the Isthmus of Panama with South America, which would have facilitated faunistic migrations across dry land between Central America and the northern Andean blocks as early as about 15 Mya (Montes et al. 2012). Consequently, the ancestral *P. caryophyllaceus* expanded into Central America during the middle Miocene. The subsequent evolution and divergence of MOTU2 and MOTU3 in eastern Panama was probably induced by eustatic fluctuations during the middle and late Miocene (as early as 11 Mya), by flooding in what are now the Atrato and Chucunaque basins; de facto separating MOTU3 on the Majé-Baudó arc (Pacific side) from MOTU2 on the Dabeiba arc (Atlantic side) (Duque-Caro 1990a, Coates & Obando 1996). Probably at least one migration has occurred from the MOTU2 and MOTU3 territory west towards the range of MOTU1, since there is evidence of the presence of all three MOTUs at El Copé in central Panama (Crawford et al. 2010, Pinto-Sánchez et al. 2012), which likely reflects a secondary contact, but for which nuclear DNA has shown neither introgression nor clear separation between the MOTUs. There might also be a remnant gene flow between MOTU1 and the MOTU3-population at Majé, since latter samples were nested within MOTU1 in the 16S tree and molecular clock (Supplementary Figs S2 + S4) with a distant divergence time of 11.12 Mya when not using the monophyly constraint for the

MOTUs in the time divergence analysis. This would mean that MOTU3 from eastern Panama had available a considerable period of time to expand into western Panama and mix with MOTU1 there.

Even though we here present a lot of new information on the distribution pattern of *Pristimantis caryophyllaceus* and its variation in morphology, genetics, colour pattern, as well as advertisement calls, it is apparently still not enough to clarify the taxonomic status of the species. Detailed molecular analyses at population level, using nuclear markers such as microsatellites to detect gene flow and past demographic bottlenecks, including populations from central Panama (especially from the Piedras-Pacora mountain range) into the analysis of morphology, and statistically supported bioacoustics data from various populations over wide areas are still needed. Further studies should include correlation analyses between geographic and genetic distances to test whether the uncovered differences express just a clinal variation among the populations, and to evaluate the existence and role of previous and current introgressions among the MOTUs, particularly at El Copé.

Acknowledgements

Scientific permits for 2009 (SC/A-8-09, SC/A-28-09), 2011 (SC/A-37-11), 2012 (SC/A-33-12), and export permits 2012 (SC/A-33-12) and 2013 (SEX/A-7-13) were provided by ANAM, Panama, and T. Quintana (Cacique General del área de Sambú) from the "Despacho del Cacique Regional" Comarca Emberá-Wounaan, Panama. Special thanks go to the indigenous people of the Embera from Puerto Indio and Pavarandó, especially to Daniel Berrugate (Secretary of the Emberá-Wounaan congress, Sambú), and Laciro Caibera (Noko of the Pavarando village) and his family who allowed us to enter their autonomous territory and kindly supported our work logistically. We are furthermore thankful to the indigenous people of the Ngöbe and Buglé, who granted us access to the Comarca Ngöbe-Buglé under permission granted by the Cacique General, Rogelio Moreno of San Félix, Panama. We are very grateful to Don Faustino, Hermelinda, and family, who gave us shelter on their nice sustainable farm at La Moneda's village during our travels to Darién. Porfírio Yangüez and Marciano Montezuma in Jurutungo supported our expedition to the Río Changena logistically. We thank Sebastian Lotzkat, Yorlis Cáceres, Isaac Pizarro, Gustavo Dogirama, Mario Cuñapa, Anselmo Caicedo, Hugo Martínez, Elacio Méndez, and Gilberto Torres for their field assistance. We thank Andrew Crawford, Jörn Köhler, and Claus Bo Petersen for insightful comments on an early draft of the manuscript. We thank Johannes Köhler for his invaluable cooperation during the lab work and data analysis, the staff of the Grunelius-Möllgaard Laboratory for Molekular Evolution, especially Heike Kappes, and Gerardo Chaves who provided pictures of the *Pristimantis educatoris* paratypes. This work was supported financially by the Secretaría de Ciencia y Tecnología (SENACYT) and Instituto para la Formación y Aprovechamiento de los Recursos Humanos (IFARHU), Panamá, and MWH, Panama. Andreas Hertz was supported financially by the FAZIT-Stiftung. The COI'5' DNA fragment was sequenced at the Southern China DNA Barcoding Center with support from the National Natural Science Foundation of China (No. 31090250), the Ministry of Science and Technology of China (Nos 2011FY120200 and 2012FY110800), and the Chinese Academy of Science (No. KSCX2-EW-Z-2).

References

Amat, F., K. C. Wollenberg & M. Vences (2013): Ecological correlates of eye colour and pattern in mantellid frogs. – Salamandra, **49**: 1–17.

Barbour, T. (1928): Proceedings of the New England Zoological Club, **10**: 28.

Batista, A. (2009): ¿Comer o Cantar? Implicaciones del tamaño corporal sobre la importancia de la dieta y el canto en un ensamble de especies de Anuros (Amphibia: Anura: Terrarana). – Unpubl. MSc thesis.

Charif, R. A., C. W. Clark & K. M. Fristrup (2004): Raven 1.3 User's Manual. – Cornell Laboratory of Ornithology, Ithaca, NY.

Clement, M., D. Posada & K. Crandall (2000): TCS: a computer program to estimate gene genealogies. – Molecular Ecology Notes, **9**: 1657–1660.

Coates, A. G. & J. A. Obando (1996): The geologic evolution of the Central American Isthmus. – pp. 21–56 in: Jackson, J. B. C., A. F. Budd & A. G. Coates (eds): Evolution and Environment in Tropical America. – University of Chicago Press, Chicago.

Coates, A. G., M. P. Aubry, W. A. Berggren, L. S. Collins & M. Kunk (2003): Early Neogene history of the Central American arc from Bocas del Toro, western Panama. – Geological Society of American Bulletin, **115**: 271–287.

Coates, A. G., L. S. Collins, M. P. Aubry & W. A. Berggren (2004): The geology of the Darien, Panama, and the late Miocene-Pliocene collision of the Panama arc with northwestern South America. – Geological Society of American Bulletin, **116**: 1327–1344.

Cope, E.D. (1885): A contribution to the herpetology of Mexico. – Proceedings of the American Philosophical Society, **22**: 380–404.

Crawford, A. J., K. R. Lips & E. Bermingham (2010): Epidemic disease decimates amphibian abundance, species diversity, and evolutionary history in the highlands of central Panama. – Proceedings of the National Academy of Sciences (USA), **107**: 13777–13782.

Crawford, A. J., C. Cruz, E. Griffith, H. Ross, R. Ibáñez, K. R. Lips, A. C. Driskell, E. Bermingham, & P. Crump (2013): DNA barcoding applied to ex situ tropical amphibian conservation programme reveals cryptic diversity in captive populations. – Molecular Ecology Resources, **13**: 1005–1018, DOI: 10.1111/1755-0998.12054

Duque-Caro, H. (1990a): Neogene stratigraphy, paleoceanography and paleobiology in northwest South America and the evolution of the Panama Seaway. – Palaeogeography, Palaeoclimatology and Palaeoecology, **77**: 203–234.

Duque-Caro, H. (1990b): The Choco Block in the northwestern corner of South America: structural, tectonostratigraphic, and paleogeographic implications. – Journal of South American Earth Sciences, **3**: 71–84.

Drummond, A. J., S. Y. W. Ho, M. J. Phillips & A. Rambaut (2006): Relaxed phylogenetics and dating with confidence. – Public Library Of Science, Biology, **4**: 699–710.

Drummond, A. J. & A. Rambaut (2007): BEAST: Bayesian evolutionary analysis by sampling trees. – BioMed Central, Evolutionary Biology, **7**: 214.

Duellman, W. E. (2001): The hylid frogs of Middle America, Vol. 2. – Contributions to Herpetology, **18**: 695–1158.

Duellman, W. E. & E. Lehr (2009): Terrestrial breeding frogs (Strabomantidae) in Peru. – Natur und Tier-Verlag, Naturwissenschaft, Münster, 384 pp.

Duellman, W. E. & L. Trueb (1994): Biology of Amphibians. – The Johns Hopkins University Press, Baltimore and London, 670 pp.

Dunn, E. R. (1937): The amphibian and reptilian fauna of bromeliads in Costa Rica and Panama. – Copeia, **1937**: 163–67.

ESRI (Environmental Systems Resource Institute) (2009): ArcMap 10. – ESRI, Redlands, California.

Farris, D. W., C. Jaramillo, G. Bayona, S. A. Restrepo-Moreno, C. Montes, A. Cardona, A. Mora, R. J. Speakman, M. D. Glascock & V. Valencia (2011): Fracturing of the Panamanian Isthmus during initial collision with South America. – Geology, **39**: 1007–1010.

Ford, E. B. (1955): Polymorphism and taxonomy. – Heredity, **9**: 255–264.

Glaw, F. & M. Vences (1997): Anuran eye colouration: definitions, variation, taxonomic implications and possible functions. – pp. 125–138 in: Böhme, W., W. Bischoff & T. Ziegler (eds): Herpetologia Bonnensis, Proceedings of the 8th Ordinary General Meeting of the Societas Europaea Herpetologica, 23–27 August 1995. – Societas Europaea Herpetologica, Deutsche Gesellschaft für Herpetologie und Terrarienkunde and Zoologisches Forschungsinstitut und Museum Alexander Koenig, Bonn.

Goin, C. J. (1950): Colour pattern inheritance in some frogs of the genus *Eleutherodactylus*. – Bulletin of the Chicago Academy of Sciences, **9**: 1–15.

Goin, C. J. (1960): Pattern variation in the frog *Eleutherodactylus nubicola* Dunn. – Bulletin of the Florida State Museum, Biological Sciences, **5**: 243–258.

Hedges, S. B., W. E. Duellman & M. P. Heinicke (2008): New World direct-developing frogs (Anura: Terrarana): Molecular phylogeny, classification, biogeography, and conservation. – Zootaxa, **1737**: 1–182.

Heinen, J. T. (1992): Comparisons of the leaf litter herpetofauna in abandoned cacao plantations and primary rain forest in Costa Rica: some implications for faunal restoration. – Biotropica, **24**: 431–439.

Heinicke, M. P., W. E. Duellman & S. B. Hedges (2007): Major Caribbean and Central American frog faunas originated by oceanic dispersal. – Proceedings of the National Academy of Sciences of the United States of America, **104**: 10092–10097.

Hoffman, E. A. & M. S. Blouin (2000): A review of colour and pattern polymorphisms in anurans. – Biological Journal of the Linnean Society, **70**: 633–665.

Huelsenbeck, J. P. & F. Ronquist (2001): MRBAYES: Bayesian inference of phylogenetic trees. – Bioinformatics, **17**: 754–755.

Köhler, G. (2011): Amphibians of Central America. – Herpeton, Germany, 379 pp.

Lieberman, S. S. (1986): Ecology of the leaf litter herpetofauna of a Neotropical rain forest La Selva, Costa Rica. – Acta Zoologica Mexicana Nueva Serie, **15**: 1–72.

Lips, K. R., J. D. Reeve & L. R. Witters (2003): Ecological traits predicting amphibian population declines in Central America. – Conservation Biology, **17**: 1078–1088.

Lynch, J. D. (1980): Systematic status and distribution of some poorly known frogs of the genus *Eleutherodactylus* from the Chocoan lowlands of South America. – Herpetologica **36**: 175–189.

Lynch, J. D. & W. E. Duellman (1997): Frogs of the genus *Eleutherodactylus* in western Ecuador. – University of Kansas Special Publication, **23**: 1–236.

Mallet, J. (2008): Hybridization, ecological races and the nature of species: empirical evidence for the ease of speciation. – Philosophical Transactions of the Royal Society B: Biological Sciences, **363**: 2971–2986.

Mayr, E. (1963): Animal species and evolution. – Cambridge, MA: Harvard University Press.

Miyamoto, M. M. (1984): Central American Frogs Allied to *Eleutherodactylus cruentus*: Allozyme and Morphological Data. – Journal of Herpetology, **18**: 256–263.

Montes, C. G., A. Bayona, A. Cardona, D. M. Buchs, C. A. Silva, S. E. Morón, N. Hoyos, D. A. Ramiréz, C. A. Jaramillo & V. Valencia (2012): Arc-continent collision and orocline formation: closing of the Central American Seaway. – Journal of Geophysical Research, **117**: DOI: 10.1029/2011JB008959.

Myers, C. W. (1969): The ecological geography of cloud forest in Panama. – American Museum Novitates, **2396**: 1–52

O'Donnell R. P. & K. E. Mock (2012): Two frog species or one? A multi-marker approach to assessing the distinctiveness of genetic lineages in the Northern Leopard Frog, *Rana pipiens*. – Conservation Genetics, **13**: 1167–1182

O'Neill, E. M. & K. H. Beard (2010): Genetic basis of a colour pattern polymorphism in the coqui frog *Eleutherodactylus coqui*. – Journal of Heredity, **101**: 703–709.

Padial, J. M. & I. De la Riva (2009): Integrative taxonomy reveals cryptic Amazonian species of *Pristimantis* (Anura: Strabomantidae). – Journal of the Linnean Society, **155**: 97–122.

Padial, J. M., A. Miralles, I. De la Riva & M. Vences (2010): The integrative future of taxonomy. – Frontiers in Zoology, **7**: 16. – http://dx.doi.org/10.1186/1742-9994-7-16.

Pianka, E.R. (1986): Ecology and Natural History of Desert Lizards. Analyses of the Ecological Niche and Community Structure. – Princeton University Press, Princeton, N.J.

Pinto-Sánchez, N. R., R. Ibáñez, S. Madriñán, O. I. Sanjur, E. Bermingham, & A. J. Crawford (2012): The Great American Biotic Interchange in frogs: Multiple and early colonization of Central America by the South American genus *Pristimantis* (Anura: Craugastoridae). – Molecular Phylogenetics and Evolution, **62**: 954–972.

Posada, D. (2008): jModelTest: Phylogenetic model averaging. – Molecular Biology and Evolution, **25**: 1253–1256.

Puillandre N, A. Lambert, S. Brouillet & G. Achaz (2011): ABGD, automatic barcode gap discovery for primary species delimitation. – Molecular Ecology, **21**: 1864–1877.

Rambaut, A., & A. Drummond (2009): Tracer 1.5. – University of Edinburgh, Edinburgh, UK, http://tree.bio.ed.ac.uk/software/tracer.

Ratnasingham S. & P. D. N. Hebert (2007): BoLD: the barcode of life data system. – Molecular Ecology Notes, **7**: 355–364.

Ryan, M. J., K. R. Lips, & J. T. Giermakowski (2010): New species of *Pristimantis* (Anura: Terrarana: Stabomantinae) from lower Central America. – Journal of Herpetology, **44**: 193–200.

Santos, J. C., L. A. Coloma, K. Summers, J. P. Caldwell, R. Ree, & D. C. Cannatella (2009): Amazonian amphibian diversity is primarily derived from Late Miocene Andean lineages. – Public Library of Science, Biology, **7**: 448–461.

Savage, J. M. (2002): The Amphibians and Reptiles of Costa Rica: A Herpetofauna between two Continents, between two Seas. – University of Chicago Press, Chicago, 934 pp.

Savage, J. M. & S. B. Emerson (1970): Central American frogs allied to *Eleutherodactylus bransfordii* (Cope): a problem of polymorphism. – Copeia, **1970**: 623–644.

Smithe, F. B. (1975–1981): Naturalist's Colour guide. Part I. Colour guide. 182 Colour swatches. – American Museum of Natural History, New York, New York, U.S.A.

Summers, K., T. W. Cronin, & T. Kennedy (2004): Cross-breeding of distinct color morphs of the strawberry poison frog (*Dendrobates pumilio*) from the Bocas del Toro Archipelago, Panama. – Journal of Herpetology, **38**: 1–8.

Tamura, K. (1992): Estimation of the number of nucleotide substitutions when there are strong transition-transversion and G + C-content biases. – Molecular Biology and Evolution, **9**: 678–687

Tamura, K., D. Peterson, N. Peterson, G. Stecher, M. Nei & S. Kumar (2011): MEGA5: Molecular Evolutionary Genetics Analysis using Maximum Likelihood, Evolutionary Distance, and Maximum Parsimony. – Molecular Biology and Evolution, **28**: 2731–2739

Vences, M., J. Köhler, D. R. Vieites & F. Glaw (2011): Molecular and bioacoustic differentiation of deep conspecific lineages of the Malagasy treefrogs *Boophis tampoka* and *B. luteus*. – Herpetology Notes, **4**: 239–246.

Vieites, D. R., K. C. Wollenberg, F. Andreone, J. Köhler, F. Glaw & M . Vences (2009): Vast underestimation of Madagascar's biodiversity evidenced by an integrative amphibian inventory. – Proceedings of the National Academy of Sciences of the United States of America, **106**: 8267–8272.

Vitt, L. J. & J. P. Caldwell (1994): Resources utilization and guild structure of small vertebrates in the Amazon forest leaf litter. – Journal of Zoology, **234**: 463–476.

Wang I. J., A. J. Crawford, & E. Bermingham (2008): Phylogeography of the Pygmy Rain Frog (*Pristimantis ridens*) across the lowland wet forests of isthmian Central America. – Molecular Phylogenetics and Evolution, **47**: 992–1004.

Webb, S. D. & A. Rancy (1996): Late Cenozoic evolution of the Neotropical mammal fauna. – pp. 335–358 in: Jackson, J. B. C., A. F. Budd & A. G. Coates (eds): Evolution and environment in tropical America. – University of Chicago, Chicago.

Weir, J. T., E. Bermingham & D. Schluter (2009): The great American biotic interchange in birds. – Proceedings of the National Academy of Sciences of the United States of America, **106**: 21737–21742.

Weimer, R., W. Feichtinger, F. Bolaños & M. Schmid (1993): Die Amphibien von Costa Rica. Herpetologische Eindrücke einer Forschungsreise. Teil III: Leptodactylidae (1). – Sauria, **15**: 19–24.

Woolbright L. L. & M. M. Stewart (2008): Spatial and temporal variation in Colour pattern morphology in the tropical frog, *Eleutherodactylus coqui*. – Copeia, **2008**: 431–437.

Supplementary material

Additional information is available in the online version of this article at http://www.salamandra-journal.com

4 Supplementary figures and 6 Supplementary tables:

Figure S1. Maximum likelihood consensus tree of the COI mtDNA of the *Pristimantis caryophyllaceus* complex.

Figure S2. Maximum likelihood consensus tree of the 16S mtDNA of the *Pristimantis caryophyllaceus* complex.

Figure S3. Maximum likelihood consensus tree of mitochondrial (16S & COI mDNA) and nuclear (RAG1 DNA) genes combined of the *Pristimantis caryophyllaceus* complex.

Figure S4. Chronogram of the *Pristimantis caryophyllaceus* complex based on Rag1, 16S and COI genes, using *P. cerasinus* and *P. cruentus* as outgroups.

Table S1. Morphological variables taken from 78 specimens used in the analyses.

Table S2. Mean genetic distances in the 16S mtDNA gene between the *Pristimantis caryophyllaceus* samples used in the phylogenetic analysis.

Table S3. Mean genetic distances in the COI mtDNA gene between the *Pristimantis caryophyllaceus* samples used in the phylogenetic analysis.

Table S4. Mean genetic distances in the COI and 16S mtDNA genes combined between the *Pristimantis caryophyllaceus* samples used in the phylogenetic analysis.

Table S5. Details of sample and museum voucher numbers.

Table S6. Transect details for *Pristimantis caryophyllaceus* (MOTU3).

Supplementary material

Batista, A., A. Hertz, G. Köhler, K. Mebert & M. Vesely: Phylogeny, shapes, colours, and phylogeography of frogs related to *Pristimantis caryophyllaceus* (Anura: Terrarana: Craugastoridae) in Panama. – Salamandra, **50**(3): 155–171.

4 Supplementary Figures and 6 Supplementary Tables.

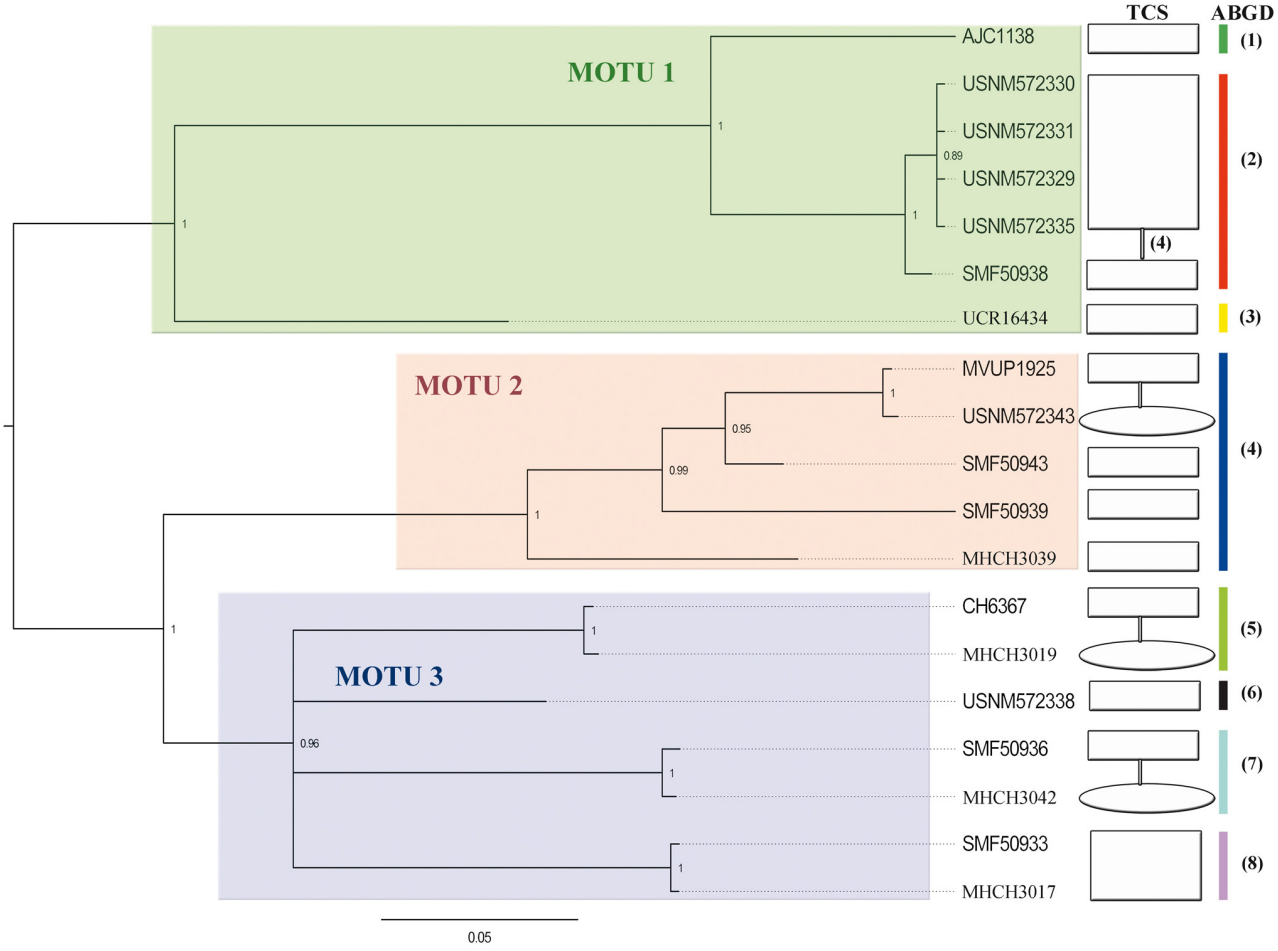

Supplementary Figure S1. Maximum likelihood consensus tree of the COI mtDNA of the *Pristimantis caryophyllaceus* complex. Specimen labels refer to collection or museum numbers. MOTU colours correspond to those in Figs. 1 and 4. Scale bar refers to the number of substitutions per site. Support of the Bayesian posterior probabilities are shown for every branch. Parsimony network with a connection limit of 90%; each node represents a unique haplotype separated from the next by one substitution step, numbers in parenthesis represents unsampled haplotypes, the rectangle the probable ancestral haplotype. ABGD colour bars represent each primary species hypothesis (number of species IDs in parenthesis), see text for details.

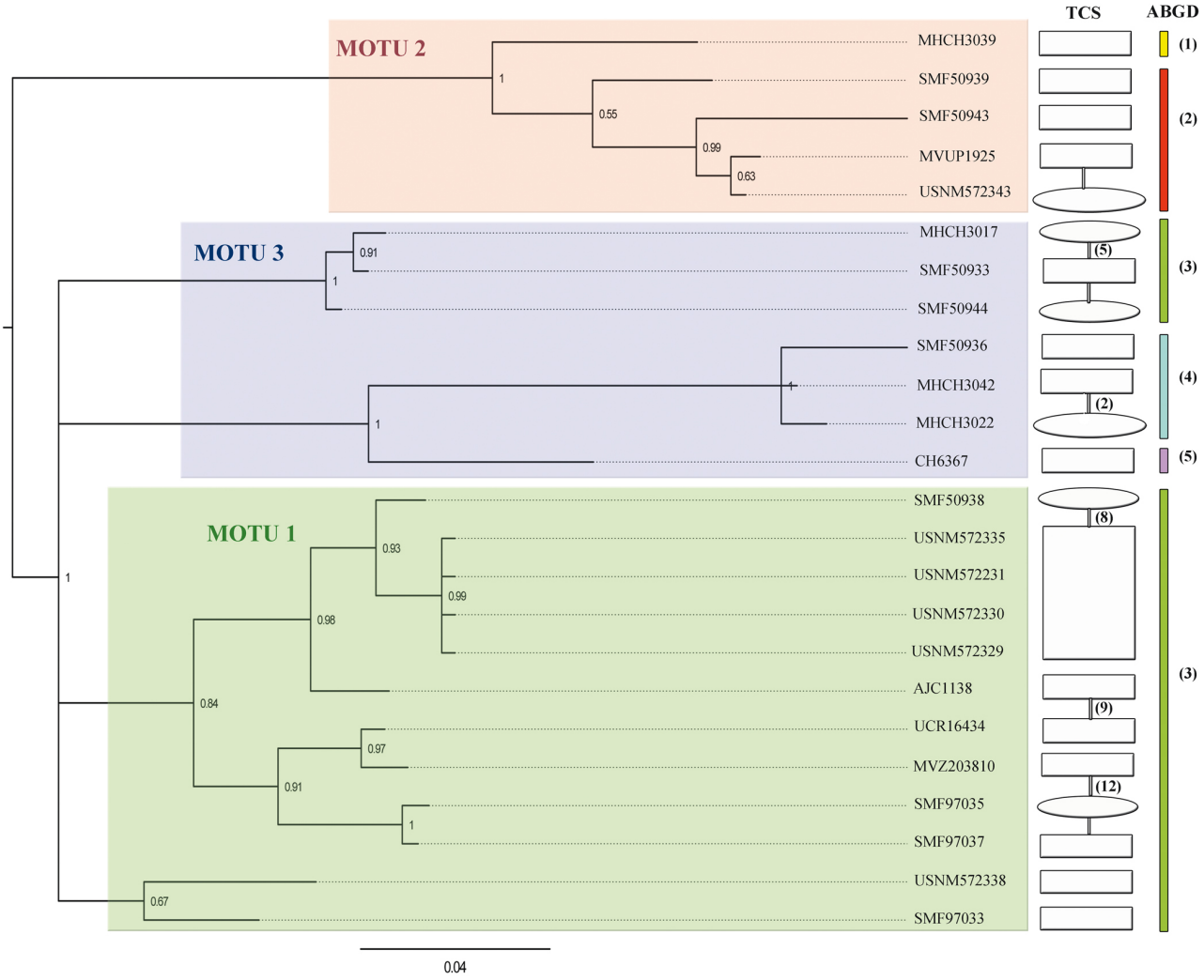

Supplementary Figure S2. Maximum likelihood consensus tree of the 16S mtDNA of the *Pristimantis caryophyllaceus* complex. Specimen labels refer to collection or museum numbers. MOTU colours correspond to those in Figures 1 and 4. Scale bar refers to the number of substitutions per site. Support of the Bayesian posterior probabilities are shown for every branch. Parsimony network with a connection limit of 90%; each node represents a unique haplotype separated from the next by one substitution step, numbers in parenthesis represents unsampled haplotypes, the rectangle the probable ancestral haplotype. ABGD colour bars represent each primary species hypothesis (number of species IDs in parenthesis), see text for details.

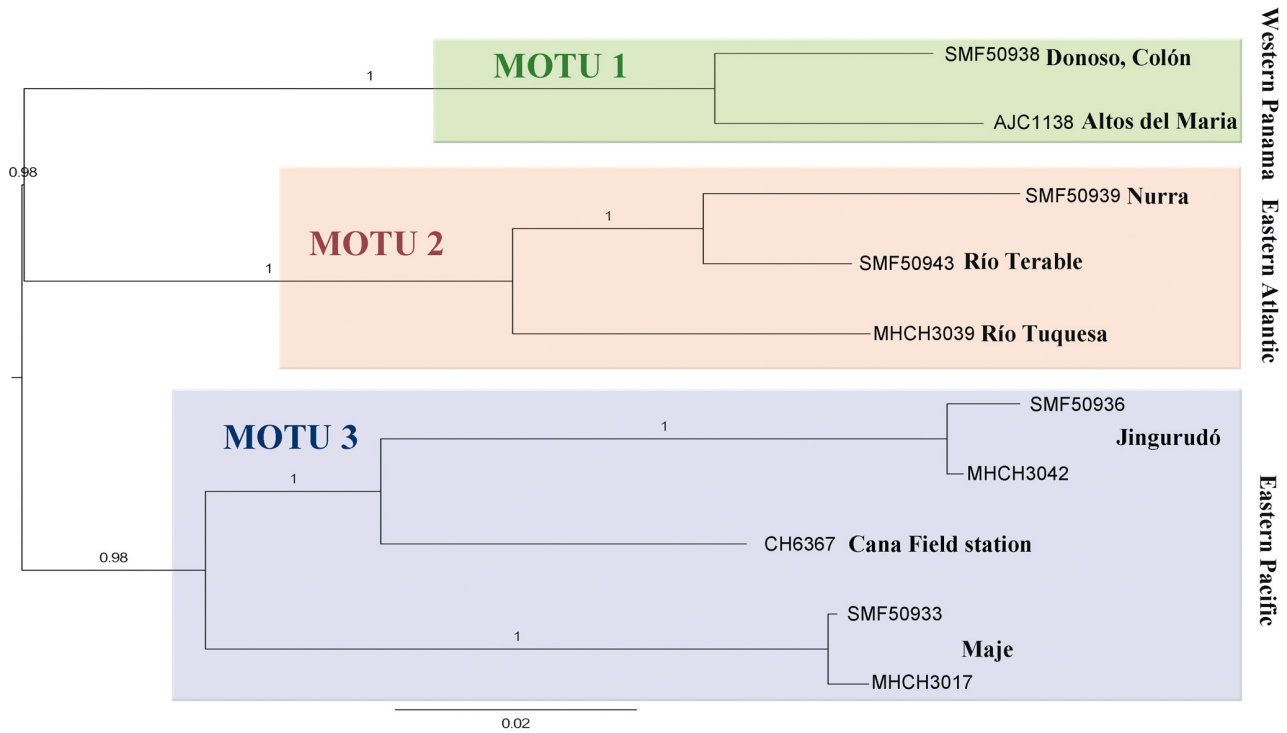

Supplementary Figure S3. Maximum likelihood consensus tree of mitochondrial (16S & COI mDNA) and nuclear (RAG1 DNA) genes combined of the *Pristimantis caryophyllaceus* complex. Specimen labels refer to collection or museum numbers. MOTUs are shadowed in the same colours as in Figures 1 and 4. Scale bar refers to number of substitutions per site. Support of the Bayesian posterior probabilities are shown for every branch.

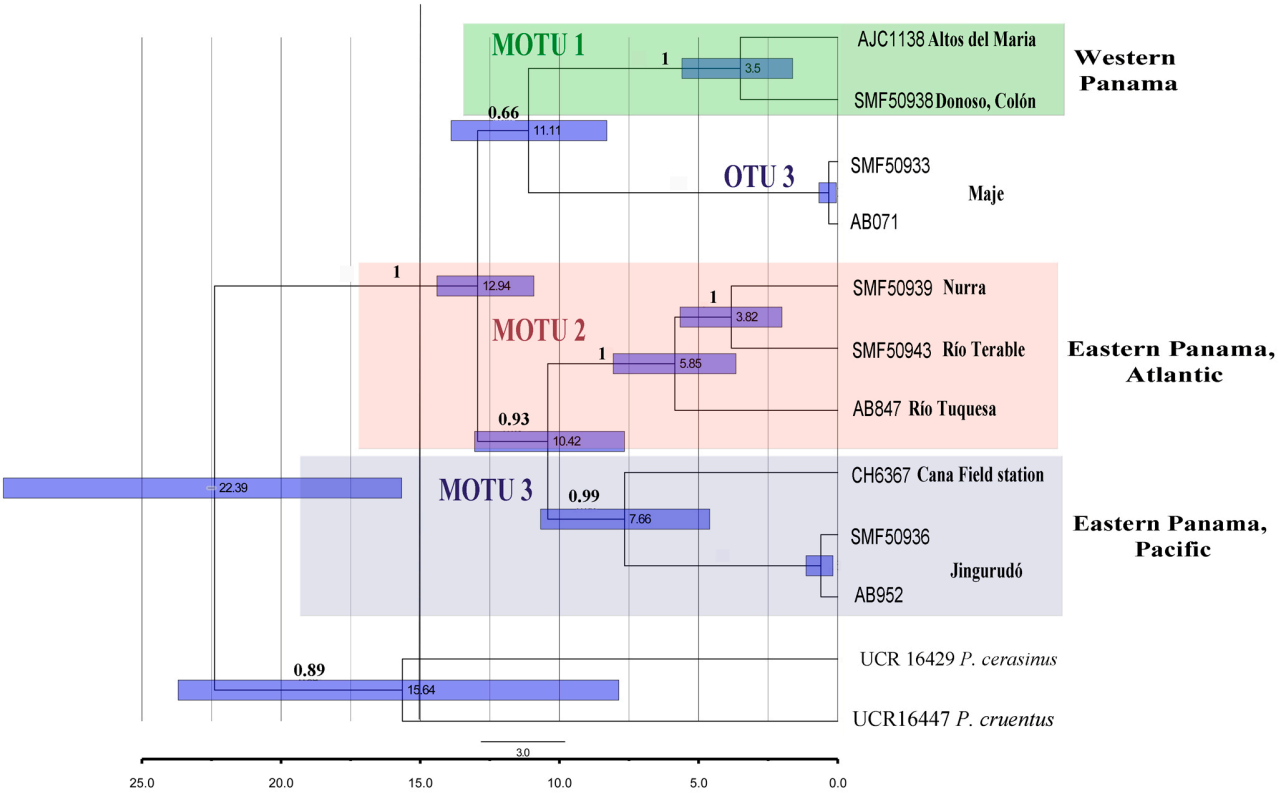

Supplementary Figure S4. Chronogram of the *Pristimantis caryophyllaceus* complex based on Rag1, 16S and COI genes, using *P. cerasinus* and *P. cruentus* as outgroups. Scale along the bottom indicates time in Mya. Block colours reflect MOTU designations (for species at tips). The vertical line indicates the hypothesized 3.5 Mya final completion of the Isthmus of Panama. Blue horizontal bars indicate 95% credibility intervals for the divergence time of the MOTUs, numbers inside the bars indicate time in Mya. Numbers above branches indicate estimated posterior probabilities ≥ 0.95 for the presence of the corresponding clade according to BEAST (see text for details).

Supplementary Table S1. Morphological variables taken from 78 specimens used in the analyses. Number of specimens measured in parenthesis (see main text for explanation).

Trait	MOTU1		MOTU2		MOTU3	
	Females (20)	Males (33)	Females (6)	Males (1)	Females (5)	Males (13)
SVL	25.53±3.09 (21.90–32.60)	20.13±1.87 (16.10–22.70)	29.02±2.56 (25.00–31.90)	22.1	29.32±1.59 (27.20–31.30)	22.54±1.83 (18.50–25.20)
HW	9.89±1.23 (8.40–13.00)	7.80±0.80 (6.30–9.40)	11.38±1.02 (10.10–12.60)	8.1	11.58±0.31 (11.10–11.90)	8.87±0.70 (7.20–10.00)
HL	9.38± 1.16 (8.10–12.30)	7.64±0.78 (6.00–9.10)	11.27±1.02 (9.60–12.40)	8.2	11.34±0.51 (10.70–12.00)	8.82±0.91 (7.10–10.10)
IND	2.03±0.28 (1.60–2.70)	1.65±0.15 (1.40–1.90)	2.38±0.16 (2.20–2.60)	1.6	2.32±0.16 (2.10–2.50)	1.94±0.12 (1.80–2.10)
IOD	3.06±0.41 (2.50–3.90)	2.49±0.29 (2.00–3.00)	3.95±0.27 (3.80–4.50)	2.9	3.94±0.40 (3.60–4.50)	3.06±0.34 (2.60–3.50)
TYMP	0.81± 0.29 (0.50–1.70)	0.69±0.14 (0.50–1.00)	1.05±0.08 (1.00–1.20)	0.8	1.16±0.23 (0.90–1.50)	1.01±0.19 (0.70–1.40)
EL	3.33±0.32 (2.90–4.10)	2.84±0.32 (2.20–3.40)	3.72±0.22 (3.40–4.00)	3.5	3.94±0.36 (3.40–4.30)	3.28±0.38 (2.50–3.80)
END	3.27±0.50 (2.60–4.60)	2.61±0.35 (2.00–3.20)	4.28±0.44 (3.70–4.90)	3.1	4.12±0.41 (3.50–4.50)	3.07±0.36 (2.50–3.60)
TL	15.03±1.72 (13.10–19.00)	12.10±1.15 (10.00–14.10)	17.47±1.01 (15.60–18.20)	12.8	17.02±0.97 (15.70–18.00)	13.28±1.07 (10.70–14.90)
FL	11.16±1.37 (9.40–14.50)	8.85±1.08 (7.00–10.90)	12.03±0.86 (10.70–13.00)	9.9	12.14±0.46 (11.40–12.50)	9.92±1.05 (7.20–11.10)
4TW	0.56±0.09 (0.50–0.90)	0.49±0.06 (0.40–0.60)	0.58±0.04 (0.50–0.60)	0.4	0.58±0.04 (0.50–0.60)	0.48±0.07 (0.40–0.60)
4TD	1.01±0.19 (0.70–1.40)	0.89±0.19 (0.60–1.30)	1.25±0.14 (1.10–1.40)	0.9	1.20±0.14 (1.00–1.40)	0.96±0.17 (0.60–1.20)
FAL	5.38±0.60 (4.50–6.80)	4.38±0.47 (3.20–5.10)	6.08±0.58 (5.60–7.20)	4.6	6.68±0.50 (5.80–7.00)	4.95±0.52 (4.10–5.70)
HAL	6.90±1.12 (5.60–9.80)	5.51±0.70 (4.40–6.90)	7.53±0.57 (6.90–8.30)	5.5	7.98±1.12 (7.20–9.90)	6.23±0.74 (4.40–7.10)
3FW	0.57±0.07 (0.50–0.70)	0.49±0.07 (0.40–0.60)	0.62±0.08 (0.50–0.70)	0.5	0.60±0.07 (0.50–0.70)	0.48±0.07 (0.40–0.60)
3FD	1.13±0.25 (0.80–1.60)	0.93±0.20 (0.60–1.40)	1.40±0.25 (1.10–1.70)	1.1	1.26±0.18 (1.10–1.50)	1.08±0.23 (0.60–1.40)
TYMP/SVL	0.03±0.01 (0.02–0.05)	0.03±0.01 (0.02–0.05)	0.04±0.01 (0.03–0.04)	0.04	0.04±0.01 (0.03–0.05)	0.04±0.01 (0.04–0.06)
TL/SVL	0.59±0.03 (0.54–0.63)	0.60±0.03 (0.51–0.66)	0.60±0.03 (0.56–0.64)	0.58	0.58±0.03 (0.54–0.62)	0.59±0.03 (0.54–)0.66
FL/SVL	0.44±0.03 (0.39–0.48)	0.44±0.03 (0.38–0.49)	0.42±0.02 (0.38–0.44)	0.45	0.35±0.17 (0.05–0.44)	0.44±0.03 (0.39–0.49)
HW/SVL	0.390.02± (0.36–0.42)	0.39±0.02 (0.36–0.44)	0.39±0.01 (0.37–0.41)	0.37	0.40±0.02 (0.38–0.41)	0.39±0.02 (0.35–0.42)
HL/SVL	0.13±0.01 (0.11–0.14)	0.13±0.01 (0.11–0.16)	0.15±0.00 (0.14–0.15)	0.14	0.14±0.02 (0.12–0.16)	0.14±0.01 (0.12–0.15)
END/SVL	0.13±0.01 (0.11–0.14)	0.13±0.01 (0.11–0.16)	0.15±0.00 (0.14–0.15)	0.14	0.14±0.02 (0.12–0.16)	0.14±0.01 (0.12–0.15)
4TD/IVTW	1.81±0.23 (1.40–2.20)	1.81±0.29 (1.40–2.60)	2.14±0.20 (1.83–2.33)	2.25	2.07±0.15 (2.00–2.33)	2.02±0.25 (1.50–2.50)
3FD/IIIFW	1.97±0.30 (1.33–2.67)	1.91±0.35 (1.33–)	2.31±0.60 (1.83–3.40)	2.2	2.11±0.26 (1.83–2.50)	2.30±0.53 (1.40–3.50)
IOD/HW	0.31±0.03 (0.27–0.38)	0.32±0.03 (0.28–0.38)	0.35±0.02 (0.33–0.38)	0.36	0.34±0.03 (0.31–0.38)	0.35±0.04 (0.28–0.42)
HL/HW	0.95±0.04 (0.85–1.01)	0.98±0.05 (0.84–1.16)	0.99±0.04 (0.94–1.06)	1.01	0.98±0.02 (0.95–1.01)	0.99±0.06 (0.91–1.11)

Supplementary Table S2. Mean genetic distances in the 16S mtDNA gene between the *Pristimantis caryophyllaceus* samples used in the phylogenetic analysis (Tamura-3-parameter-distances).

		1	2	3	4	5	6	7	8	9	10	11	12	13	14	15	16	17	18	19	20	21	22	23
1	USNM572335 {MOTU1}																							
2	USNM572331 {MOTU1}	0.0																						
3	AJC1138 {MOTU1}	2.8	2.8																					
4	UCR16434 {MOTU1}	4.3	4.3	3.3																				
5	USNM572330 {MOTU1}	0.0	0.0	2.8	4.3																			
6	SMF97035 {MOTU1}	6.3	6.3	5.2	3.8	6.3																		
7	SMF 97037 {MOTU1}	6.3	6.3	5.2	3.8	6.3	0.0																	
8	USNM572329 {MOTU1}	0.0	0.0	2.8	4.3	0.0	6.3	6.3																
9	MVZ203810 {MOTU1}	4.8	4.8	3.8	0.5	4.8	4.3	4.3	4.8															
10	SMF50938 {MOTU1}	1.4	1.4	2.3	3.8	1.4	5.8	5.8	1.4	4.3														
11	MHCH3039 {MOTU2}	7.3	7.3	7.3	5.8	7.3	8.3	8.3	7.3	6.3	6.8													
12	SMF50939 {MOTU2}	7.3	7.3	6.2	6.8	7.3	7.8	7.8	7.3	7.3	6.8	2.3												
13	USNM572343 {MOTU2}	7.3	7.3	7.3	6.2	7.3	7.8	7.8	7.3	6.7	6.8	2.3	1.9											
14	MVUP1925 {MOTU2}	7.3	7.3	7.3	6.2	7.3	7.8	7.8	7.3	6.7	6.8	2.3	1.9	0.0										
15	SMF50943 {MOTU2}	7.8	7.8	7.8	6.7	7.8	8.3	8.3	7.8	7.3	7.3	1.9	1.4	0.5	0.5									
16	SMF50933 {MOTU3}	4.7	4.7	5.7	4.3	4.7	7.3	7.3	4.7	4.8	5.2	6.3	7.8	7.8	7.8	8.3								
17	MHCH3022 {MOTU3}	9.3	9.3	9.3	9.3	9.3	10.4	10.4	9.3	9.9	8.8	9.8	9.8	9.8	9.8	10.3	8.8							
18	MHCH3017 {MOTU3}	5.2	5.2	6.2	4.8	5.2	7.8	7.8	5.2	5.3	5.7	6.8	8.3	8.3	8.3	8.8	0.5	9.3						
19	SMF50936 {MOTU3}	9.8	9.8	9.9	8.8	9.8	9.9	9.9	9.8	9.4	10.4	11.5	11.4	11.4	11.4	12.0	8.8	2.3	9.3					
20	MHCH3042 {MOTU3}	8.8	8.8	8.8	8.8	8.8	9.9	9.9	8.8	9.4	8.3	9.3	9.3	9.3	9.3	9.8	8.3	0.5	8.8	1.9				
21	SMF50944 {MOTU3}	4.7	4.7	5.7	4.3	4.7	7.3	7.3	4.7	4.8	5.2	6.3	7.8	7.8	7.8	8.3	0.0	8.8	0.5	8.8	8.3			
22	CH6367 {MOTU3}	7.8	7.8	6.7	7.8	7.8	7.8	7.8	7.8	8.3	7.2	8.3	7.2	8.2	8.2	8.8	7.7	6.2	8.3	7.8	5.8	7.7		
23	SMF97033 {MOTU1}	3.8	3.8	4.8	4.8	3.8	7.8	7.8	3.8	5.3	4.3	6.3	6.8	6.8	6.8	7.3	3.8	9.9	4.3	10.4	9.3	3.8	8.8	
24	USNM572338 {MOTU1}	4.8	4.8	4.7	4.7	4.8	6.7	6.7	4.8	5.2	5.3	5.7	6.3	6.2	6.2	6.8	4.7	10.9	5.2	11.4	10.4	4.7	9.3	3.8

Supplementary Table S3. Mean genetic distances in the COI mtDNA gene between the *Pristimantis caryophyllaceus* samples used in the phylogenetic analysis (Tamura-3-parameter-distances).

		1	2	3	4	5	6	7	8	9	10	11	12	13	14	15	16	17	18
1	USNM572331 {MOTU1}	0.0																	
2	USNM572330 {MOTU1}	0.0																	
3	USNM572329 {MOTU1}	0.0	0.0																
4	SMF50938 {MOTU1}	0.9	0.9	0.9															
5	USNM572335 {MOTU1}	0.0	0.0	0.0	0.9														
6	UCR16434 {MOTU1}	16.4	16.4	16.4	15.9	16.4													
7	AJC1138 {MOTU1}	8.4	8.4	8.4	8.2	8.4	16.9												
8	MHCH3039 {MOTU2}	20.1	20.1	20.1	20.4	20.1	16.9	21.5											
9	SMF50939 {MOTU2}	22.0	22.0	22.0	21.8	22.0	17.7	21.5	11.4										
10	SMF50943 {MOTU2}	20.1	20.1	20.1	20.1	20.1	14.6	20.9	8.8	6.9									
11	MVUP1925 {MOTU2}	19.8	19.8	19.8	19.8	19.8	16.2	21.2	9.8	8.0	4.4								
12	USNM572343 {MOTU2}	20.1	20.1	20.1	20.1	20.1	16.4	20.9	10.1	8.2	4.6	0.2							
13	SMF50933 {MOTU3}	19.7	19.7	19.7	20.5	19.7	15.5	20.5	16.6	17.3	16.8	17.0	17.3						
14	MHCH3042 {MOTU3}	19.3	19.3	19.3	19.3	19.3	15.9	20.3	14.8	17.7	14.8	15.8	16.0	12.3					
15	CH6367 {MOTU3}	17.0	17.0	17.0	17.5	17.0	14.1	19.5	13.9	16.0	13.7	14.6	14.8	11.6	11.5				
16	USNM572338 {MOTU3}	17.2	17.2	17.2	17.2	17.2	13.5	17.2	15.8	17.7	14.4	15.0	15.3	10.5	10.3	11.1			
17	MHCH3017 {MOTU3}	19.7	19.7	19.7	20.5	19.7	15.5	20.5	16.6	17.3	16.8	17.0	17.3	0.0	12.3	11.6	10.5		
18	SMF50936 {MOTU3}	18.8	18.8	18.8	18.8	18.8	15.5	19.8	15.3	17.7	14.8	15.8	16.0	12.3	0.4	12.0	10.3	12.3	
19	MHCH3019 {MOTU3}	17.2	17.2	17.2	17.7	17.2	14.3	19.7	13.7	15.7	13.4	14.3	14.6	11.8	11.8	0.2	11.3	11.8	12.2

Supplementary Table S4. Mean genetic distances in the COI and 16S mtDNA genes combined between the *Pristimantis caryophyllaceus* samples used in the phylogenetic analysis.

		1	2	3	4	5	6	7	8	9	10	11	12	13	14	15	16	17
1	USNM572329 {MOTU1}																	
2	AJC1138 {MOTU1}	6.8																
3	UCR16434 {MOTU1}	12.7	12.7															
4	USNM572335 {MOTU1}	0.0	6.8	12.7														
5	USNM572331 {MOTU1}	0.0	6.8	12.7	0.0													
6	USNM572330 {MOTU1}	0.0	6.8	12.7	0.0	0.0												
7	SMF50938 {MOTU1}	1.1	6.5	12.2	1.1	1.1	1.1											
8	CH6367 {MOTU3}	14.2	15.6	12.3	14.2	14.2	14.2	14.4										
9	MHCH3017 {MOTU3}	15.2	16.1	12.3	15.2	15.2	15.2	15.9	10.6									
10	SMF50936 {MOTU3}	16.1	16.8	13.5	16.1	16.1	16.1	16.3	10.8	11.4								
11	MHCH3042 {MOTU3}	16.1	16.9	13.8	16.1	16.1	16.1	16.0	9.8	11.2	0.8							
12	SMF50933 {MOTU3}	15.1	15.9	12.1	15.1	15.1	15.1	15.7	10.5	0.1	11.2	11.1						
13	USNM572338 {MOTU3}	13.4	13.4	10.9	13.4	13.4	13.4	13.6	10.6	8.9	10.6	10.3	8.8					
14	MVUP1925 {MOTU2}	16.0	16.9	13.2	16.0	16.0	16.0	15.8	12.7	14.4	14.5	13.8	14.2	12.4				
15	MHCH3039 {MOTU2}	16.2	17.1	13.6	16.2	16.2	16.2	16.2	12.2	13.6	14.2	13.2	13.5	12.8	7.6			
16	SMF50943 {MOTU2}	16.4	16.9	12.2	16.4	16.4	16.4	16.2	12.2	14.4	14.0	13.4	14.3	12.1	3.2	6.7		
17	USNM572343 {MOTU2}	16.2	16.7	13.4	16.2	16.2	16.2	16.0	12.9	14.6	14.6	14.0	14.4	12.6	0.1	7.8	3.4	
18	SMF50939 {MOTU2}	17.5	16.8	14.4	17.5	17.5	17.5	17.1	13.3	14.6	15.8	15.2	14.4	14.2	6.2	8.7	5.3	6.3

Supplementary Table S5. Details of sample and museum voucher numbers (where available), collecting localities, and GenBank accession numbers for all samples used in this study.

Voucher	Species	Locality	Province	Country	Genbank accession number			Coordinates		elev. (m)
					16S	COI	RAG1	N	W	
AJC1138	*P. caryophyllaceus**	Panama, corregimiento de Chame, Altos del Maria, ~7.5 km NE of El Valle de Anton, corregimiento, Chame	Panama	Panama	JN991435.1	JN991364	JQ025176	8.6330	-80.0770	
CH6367	*P. caryophyllaceus**	Panama, Darién, Distrito de Pinogana, Cana, Laguna	Darién	Panama	JN991436.1	JN991365	JQ025175	7.7220	-77.6560	
MHCH3183	*P. caryophyllaceus*	Fortuna/Westhang Pata de Macho	Chiriquí	Panama				8.6710	-82.1967	1420
MHCH3184	*P. caryophyllaceus*	Fortuna/Westhang (=western slope) Pata de Macho	Chiriquí	Panama				8.6710	-82.1967	1420
MHCH3185	*P. caryophyllaceus*	Fortuna/Westhang (=western slope) Pata de Macho	Chiriquí	Panama				8.6775	-82.1980	1760
MHCH3186	*P. caryophyllaceus*	La Nevera/Cerro Santiago Westhang (=western slope)	Comarca Ngöbe Buglé	Panama				8.5011	-81.7694	1580
MHCH3187	*P. caryophyllaceus*	La Nevera/Cerro Santiago Westhang (=western slope)	Comarca Ngöbe Buglé	Panama				8.5010	-81.7691	1600
MHCH3188	*P. caryophyllaceus*	La Nevera/Cerro Santiago Westhang (=western slope)	Comarca Ngöbe Buglé	Panama				8.5010	-81.7691	1600
MHCH3189	*P. caryophyllaceus*	Cerro Mariposa	Veraguas	Panama				8.5145	-81.1207	880
MHCH3190	*P. caryophyllaceus*	Cerro Mariposa, Santa Fe	Veraguas	Panama				8.5122	-81.1214	935
MHCH3191	*P. caryophyllaceus*	Cerro Mariposa, Santa Fe	Veraguas	Panama				8.5001	-81.1170	1255
MHCH3192	*P. caryophyllaceus*	Cerro Mariposa, Santa Fe	Veraguas	Panama				8.5001	-81.1173	1261
MHCH3193	*P. caryophyllaceus*	Cerro Mariposa, Santa Fe	Veraguas	Panama				8.5111	-81.1214	916
MHCH3194	*P. caryophyllaceus*	Fortuna	Chiriquí	Panama				8.6739	-82.2188	1292
MHCH3017	*P. caryophyllaceus*	Serrania de Majé, Ambroya, Chepo	Panamá	Panama	KJ201960	KJ201949	KJ201970	8.8921	-78.5604	911
MHCH3018	*P. caryophyllaceus*	Serrania de Majé, Ambroya, Chepo	Panamá	Panama				8.8916	-78.5617	886
MHCH3019	*P. caryophyllaceus*	Panama, Darién, Distrito de Pinogana, Cana, Laguna	Darién	Panama	KJ201961	KJ201950				
MHCH3020	*P. caryophyllaceus*	Río Sambu, Serranía de Jingurudo, Sambú.	Darién	Panama				7.6842	-78.0387	971
MHCH3021	*P. caryophyllaceus*	Cerro Sapo, Garachiné	Darién	Panama				7.9762	-78.3626	1169
MHCH3022	*P. caryophyllaceus*	Cerro Sapo, Garachiné	Darién	Panama	KJ201952	KJ201942		7.9762	-78.3628	1168
MHCH3037	*P. caryophyllaceus*	Río Taintidu, Chucunaque	Wargandi	Panama				9.0355	-78.0264	289
MHCH3038	*P. caryophyllaceus*	Río Taintidu, Chucunaque	Wargandi	Panama				9.0593	-77.9842	553
MHCH3039	*P. caryophyllaceus*	Río Tuquesa, Embera-Waounaan	Embera-Wounaan	Panama			KJ201967	8.4800	-77.5194	859
MHCH3040	*P. caryophyllaceus*	Río Tuquesa, Embera-Waounaan	Embera-Wounaan	Panama				8.4791	-77.5280	718
MHCH3041	*P. caryophyllaceus*	Río Tuquesa, Embera-Waounaan	Embera-Wounaan	Panama				8.4791	-77.5280	718
MHCH3042	*P. caryophyllaceus*	Río Sambu, Serranía de Jingurudo, Sambú.	Embera-Wounaan	Panama			KJ201969	7.7640	-78.1006	655
MHCH3043	*P. caryophyllaceus*	Chucantí ridge, río Congo, Chepigana	Darién	Panama				8.7977	-78.4623	1295
MHCH3044	*P. caryophyllaceus*	Chucantí ridge, río Congo, Chepigana	Darién	Panama				8.7965	-78.4630	1342
MHCH3045	*P. caryophyllaceus*	Rancho Frío Field station, Pinogana	Darién	Panama				7.9595	-77.7037	1230
MHCH3046	*P. caryophyllaceus*	Rancho Frío Field station, Pinogana	Darién	Panama				7.9595	-77.7037	1230
MHCH457	*P. caryophyllaceus*	El pianista, Bocas del Toro, Panamá	Bocas del Toro	Panama				8.8714	-82.4159	
MHCH523	*P. caryophyllaceus*	Qda Arena, Fortuna, Chiriquí, Panamá	Chiriquí	Panama				8.7180	-82.2284	1074
MVUP1925	*P. caryophyllaceus**	Parque Nacional G. D. Omar Torrijos H., El Cope, Corregimiento is Ola, Distrito La Pintada, Coclé	Coclé	Panama	FJ784473.1	FJ766776		8.6670	-80.5920	800

Voucher	Species	Locality	Province	Country	Genbank accession number			Coordinates		elev. (m)
					16S	COI	RAG1	N	W	
MVZ203810	*P. caryophyllaceus**	Costa Rica: Cartago, 2.5 km S Tapanti Bridge across Rio Grande de Orosi	Cartago	Costa Rica	EU186686.1	na				
SMF 89976	*P. caryophyllaceus*	Cerro Negro/PN Santa Fe	Veraguas	Panama				8.5706	-81.1043	800
SMF 89977	*P. caryophyllaceus*	Cerro Negro/PN Santa Fe	Veraguas	Panama				8.5663	-81.0988	690
SMF 89978	*P. caryophyllaceus*	Cerro Negro/PN Santa Fe	Veraguas	Panama				8.5706	-81.1043	800
SMF 89979	*P. caryophyllaceus*	Cerro Negro/PN Santa Fe	Veraguas	Panama				8.5769	-81.0973	900
SMF 89980	*P. caryophyllaceus*	Cerro Mariposa	Veraguas	Panama				8.6757	-81.1228	1385
SMF 89981	*P. caryophyllaceus*	I Brazo Mulaba	Veraguas	Panama				8.5186	-81.1332	700
SMF 97027	*P. caryophyllaceus*	La Nevera		Panama				8.4996	-81.7710	1650
SMF 97028	*P. caryophyllaceus*	Cerro Mariposa	Veraguas	Panama				8.5145	-81.1207	880
SMF 97029	*P. caryophyllaceus*	La Nevera/Cerro Santiago Westhang	Comarca Ngöbe Buglé	Panama				8.4953	-81.7673	1800
SMF 97030	*P. caryophyllaceus*	Llano Tugri	Comarca Ngöbe Buglé	Panama				8.5082	-81.7162	1600
SMF 97031	*P. caryophyllaceus*	Willi Mazu	Comarca Ngöbe Buglé	Panama				8.7885	-82.2016	799
SMF 97032	*P. caryophyllaceus*	Willi Mazu	Comarca Ngöbe Buglé	Panama				8.7885	-82.2016	799
SMF 97033	*P. caryophyllaceus*	Willi Mazu	Comarca Ngöbe Buglé	Panama	KJ476734			8.7885	-82.2016	799
SMF 97034	*P. caryophyllaceus*	Changena Trail/Oberes Camp	Bocas del Toro	Panama				8.9505	-82.7094	1968
SMF 97035	*P. caryophyllaceus*	Changena Trail/Oberes Camp	Bocas del Toro	Panama	KJ476733			8.9505	-82.7094	1968
SMF 97036	*P. caryophyllaceus*	Rio Clarito	Bocas del Toro	Panama				9.0090	-82.6644	1258
SMF 97037	*P. caryophyllaceus*	Rio Clarito	Bocas del Toro	Panama	KJ476732			9.0090	-82.6644	1258
SMF 97039	*P. caryophyllaceus*	Cerro Guayaba	Chiriquí	Panama				8.7657	-82.2528	1565
SMF 97040	*P. caryophyllaceus*	Cerro Mariposa, Santa Fe	Veraguas	Panama				8.5122	-81.1214	935
SMF 97041	*P. caryophyllaceus*	Cerro Mariposa, Santa Fe	Veraguas	Panama				8.5061	-81.1196	1108
SMF 97042	*P. caryophyllaceus*	Cerro Mariposa, Santa Fe	Veraguas	Panama				8.4966	-81.1164	1356
SMF 97043	*P. caryophyllaceus*	Cerro Mariposa, Santa Fe	Veraguas	Panama				8.4997	-81.1168	1264
SMF 97044	*P. caryophyllaceus*	Cerro Mariposa, Santa Fe	Veraguas	Panama				8.5000	-81.1170	1257
SMF 97045	*P. caryophyllaceus*	Cerro Mariposa, Santa Fe	Veraguas	Panama				8.5000	-81.1170	1257
SMF 97046	*P. caryophyllaceus*	Cerro Mariposa, Santa Fe	Veraguas	Panama				8.5024	-81.1191	1163
SMF 97047	*P. caryophyllaceus*	Lost and Found/Fortuna	Chiriquí	Panama				8.6757	-82.2128	1364
SMF 97048	*P. caryophyllaceus*	Lost and Found/Fortuna	Chiriquí	Panama				8.6773	-82.2103	1288
SMF50931	*P. caryophyllaceus*	Serrania de Maje, Ambroya, Chepo	Panamá	Panama				8.8920	-78.5609	901
SMF50932	*P. caryophyllaceus*	Serrania de Maje, Ambroya, Chepo	Panamá	Panama				8.8920	-78.5609	901
SMF50933	*P. caryophyllaceus*	Serrania de Maje, Ambroya, Chepo	Panamá	Panama	KJ201953	KJ201943	KJ201963	8.8919	-78.5608	911
SMF50934	*P. caryophyllaceus*	Rancho Frío Field station, Pinogana	Darién	Panama				7.9891	-77.7073	1136
SMF50935	*P. caryophyllaceus*	Río Sambu, Serranía de Jingurudo, Sambú.	Darién	Panama				7.6841	-78.0387	962
SMF50936	*P. caryophyllaceus*	Río Sambu, Serranía de Jingurudo, Sambú.	Darién	Panama	KJ201954	KJ201944	KJ201964	7.6837	-78.0384	961
SMF50937	*P. caryophyllaceus*	Río Sambu, Serranía de Jingurudo, Sambú.	Darién	Panama				7.6691	-78.0380	1133
SMF50938	*P. caryophyllaceus*	Qda Valle Grande, Donoso	Colón	Panama	KJ201958	KJ201947	KJ201968	8.8216	-80.6632	211

Voucher	Species	Locality	Province	Country	Genbank accession number			Coordinates		elev. (m)
					16S	COI	RAG1	N	W	
SMF50939	*P. caryophyllaceus*	Río Taintidu, Chucunaque	Wargandi	Panama	KJ201962	KJ201951	KJ201971	9.0355	-78.0264	289
SMF50940	*P. caryophyllaceus*	Río Taintidu, Chucunaque	Wargandi	Panama				9.0355	-78.0264	289
SMF50941	*P. caryophyllaceus*	Serranía de San Blas	Guna Yala	Panama				9.0611	-77.9797	340
SMF50942	*P. caryophyllaceus*	Río Sambu, Serranía de Jingurudo, Sambú	Embera-Wounaan	Panama				7.7590	-78.0923	643
SMF50943	*P. caryophyllaceus*	Río Terable, El Llano, Chepo	Panama	Panama			KJ201965	9.2840	-78.9838	322
SMF50944	*P. caryophyllaceus*	Chucantí ridge, río Congo, Chepigana	Darién	Panama	KJ201956		KJ201966	8.7977	-78.4623	1295
SMF50945	*P. caryophyllaceus*	Chucantí ridge, río Congo, Chepigana	Darién	Panama				8.7977	-78.4623	1295
SMF50946	*P. caryophyllaceus*	Rancho Frío Field station, Pinogana	Darién	Panama				8.0168	-77.7297	133
SMF50947	*P. caryophyllaceus*	Rancho Frío Field station, Pinogana	Darién	Panama				7.9595	-77.7037	1230
SMF85008	*P. caryophyllaceus*	RF Fortuna	Chiriquí	Panama				8.7264	-82.2615	1100
SMF85010	*P. caryophyllaceus*	RF Fortuna	Chiriquí	Panama				8.7264	-82.2615	1100
SMF85011	*P. caryophyllaceus*	RF Fortuna	Chiriquí	Panama				8.7264	-82.2615	1100
SMF85012	*P. caryophyllaceus*	RF Fortuna	Chiriquí	Panama				8.7264	-82.2615	1100
SMF85014	*P. caryophyllaceus*	BP Palo seco, Los tucanes trail	Bocas del Toro	Panama				8.7817	-82.2122	1120
SMF85015	*P. caryophyllaceus*	Fortuna Town	Chiriquí	Panama				8.7313	-82.2534	1300
SMF85016	*P. caryophyllaceus*	La Nevera	Comarca Ngöbe Buglé	Panama				8.4996	-81.7710	1600
SMF85018	*P. caryophyllaceus*	La Nevera	Comarca Ngöbe Buglé	Panama				8.4996	-81.7710	1600
UCR 16429	*P. cerasinus**	Vuelta de Queque, Rio Siquirres trail, Guayacan	Limón	Costa Rica	JN991437	JN991366	JQ025177	10.0400	-83.5500	
UCR16434	*P. caryophyllaceus**	Costa Rica: San Jose, Rio Gacho, Los Juncos, Cascajal, Canton Vazquez de Coronado	San José	Costa Rica	JN991434.1	JN991363		9.9800	-83.8400	
UCR16447	*P. cruentus**	Tapantí, Cantón, Paraiso	Cartago	Costa Rica	JN991441	JN991370	JQ025179	9.6500	-83.8500	1200
USNM572329	*P. caryophyllaceus**	Parque Nacional G. D. Omar Torrijos H., El Cope, Corregimiento is Ola, Distrito La Pintada, Cocle	Coclé	Panama	FJ784397.1	FJ766771		8.6670	-80.5920	800
USNM572330	*P. caryophyllaceus**	Parque Nacional G. D. Omar Torrijos H., El Cope, Corregimiento is Ola, Distrito La Pintada, Cocle	Coclé	Panama	FJ784421.1	FJ766774		8.6670	-80.5920	800
USNM572331	*P. caryophyllaceus**	Parque Nacional G. D. Omar Torrijos H., El Cope, Corregimiento is Ola, Distrito La Pintada, Cocle	Coclé	Panama	FJ784422.1	FJ766773		8.6670	-80.5920	800
USNM572335	*P. caryophyllaceus**	Parque Nacional G. D. Omar Torrijos H., El Cope, Corregimiento is Ola, Distrito La Pintada, Cocle	Coclé	Panama	FJ784589.1	FJ766770		8.6670	-80.5920	800
USNM572338	*P. caryophyllaceus**	Parque Nacional G. D. Omar Torrijos H., El Cope, Corregimiento is Ola, Distrito La Pintada, Cocle	Coclé	Panama	FJ784491.1	FJ766775		8.6670	-80.5920	800
USNM572343	*P. caryophyllaceus**	Parque Nacional G. D. Omar Torrijos H., El Cope, Corregimiento is Ola, Distrito La Pintada, Cocle	Coclé	Panama	FJ784375.1	FJ766772		8.6670	-80.5920	800
GK1452	*P. caryophyllaceus*	RF Fortuna	Chiriquí	Panama				8.7264	-82.2615	1100
GK1469	*P. caryophyllaceus*	BP Palo seco Los tucanes	Bocas del Toro	Panama				8.7817	-82.2122	1120
GK1595	*P. caryophyllaceus*	La nevera	Comarca Ngöbe Buglé	Panama				8.4996	-81.7710	1600

Supplementary Table S6. Transect details for *Pristimantis caryophyllaceus* (MOTU3).

Locality	Indiv.	Date	Length (m)	Duration	Climatic condition	T (°C)	Humidity (%)	Altitude (m)	Coordinates N	W
Serrania de Pirre	8	10/08/2011	240	03:30:00	cloudy	22.3	76	1137	7.98845	77.7076
Serrania de Pirre	10	11/08/2011	300	02:53:45	rainy	20.5	79	1110	7.9791	77.7086
Serrania de Jingurudó	7	26/09/2011	200	03:20:00	clear	20.9	84	943	7.68338	78.0384
Serrania de Jingurudó	8	27/09/2011	418	03:46:00	clear	23.5	79	953	7.68035	78.0387
Serrania de Jingurudó	3	29/09/2011	280	03:00:00	cloudy	22.6	81	865	7.69312	78.0423
Serrania de Sapo	4	05/12/2011	172	03:10:00	cloudy	21.4	72	1160	7.97589	78.3625
Serrania de Sapo	6	06/12/2011	160	03:50:00	cloudy	19.4	83	917	7.97749	78.3592

Supplementary Text S6. *Pristimantis caryophyllaceus* complex colour descriptions.

MOTU1: Alto de Piedra, Veraguas (MHCH3189, no photo): Dorsal base colour Buff (124) with dark Brownish Olive (129) v-shaped transversal stripes and dark Brownish Olive (129) mottling in between. Posterior surface of thigh Gem Ruby (110). Ventral surface Salmon Colour (106) with small dark spots in the gular region and small white spots between axilla and groin.

Reserva Forestal La Fortuna, western slope of Cerro Pata de Macho, Chiriquí (MHCH3184): Dorsal base colour Cinnamon (123A) with a suggestion of Yellow Ochre (123C), bordered by Sepia (119); dorsal tubercles Buff Yellow (53); lateral surfaces transparent lgc sparsely mottled with Buff Yellow (53) and fading dorsally into Buff Yellow (53) on transparent ground; dlc dorsal surfaces of limbs Buff Yellow (53) on transparent ground speckled with Olive-Green (Auxiliary) (47) auxiliary lines; vgc ventral ground colour dirty white fading into Smalt Blue (70) towards lateral edges; vlc ventral surfaces of hands and feet transparent with spots of Buff Yellow (53), and tubercles in Sepia (119); Ic Iris colouration Pale Pinkish Buff (121D), bordered with Sepia (119) and Robin's Egg Blue (93).

MOTU2: Río Tuquesa, Darién Mountain Range (MHCH3039, Fig. 8E): Dorsal colour Chamois (84) with Warm Sepia (40) irregular blotches and spots; Warm Sepia (40) interorbital band; upper surface of thigh with Warm Sepia (40) bars; groin and posterior surface of thigh suffused with Geranium (66); upper iris region Medium Chrome Orange (75); lower iris region Cream White (52), iris centre Dark Salmon (59); iris periphery Jet Black (300); eye periphery Smoky White (261).

Nurra, San Blas Mountain range (SMF50939, Fig 8G): Dorsal colour Russet (44) with small Warm Sepia (40) spots; upper surface of thigh with Pale Pinkish Buff (3) bars; groin and posterior surface of thigh suffused with Geranium (66); upper iris region Spectrum Orange (9); lower iris region Light Lavender (201), iris centre Dark Salmon (59); iris periphery Jet Black (300); eye periphery Pearl Gray (262). SMF50940 (Fig. 8H) same as SMF50939, but with the upper and lower iris regions Spectrum Red (67), and the eye periphery Light Sky Blue (191).

Nurra, San Blas mountain range (MHCH3037, Juvenile, Fig. 8F): Dorsal colour Sepia (279) with a mid-dorsal line in Medium Fawn (257); a series of delicate Medium Fawn (257) transverse lines on dorsum; dorsolateral line from the tip of snout to the groin Beige (254); upper and lower iris regions Spectrum Red (67); iris periphery Jet Black (300); eye periphery Pearl Gray (262).

MOTU3: Pirre Mountain range (SMF50934, 1149): Dorsal colour Buff (5), frontal region and some blotches on the rest of the dorsum Pale Buff (1); no contrasting pattern on groin or posterior surface of thigh; upper and lower iris regions Light Buff (2), iris centre Walnut Brown (27); iris periphery Jet Black (300); eye periphery Smoky White (261).

Pirre mountain range (SMF50946, Fig. 9F) Dorsal colour Buff (5), with small, scattered black spots; Pale Buff (1) spots on dorsum; no contrasting pattern on groin or posterior surface of thigh; upper and lower iris regions Light Buff (2), iris centre Walnut Brown (27); iris periphery Jet Black (300); eye periphery Smoky White (261).

Pirre Mountain range (MHCH3045, Fig. 9G): Dorsal colour Raw Umber (22) with a Light Yellow Ochre (13) dorsolateral line from the tip of the snout to the groin, separating the dorsal from the lateral colouration; face Tawny Olive (17), lateral region behind the eyes Light Yellow Ochre (13); groin and posterior surface of thigh Buff Yellow (6); upper surface of thigh with Ground Cinnamon (270) bars. Upper and lower iris region Light Buff (2); iris centre Walnut Brown (27); iris periphery Jet Black (300); eye periphery Smoky White (261).

Cerro Garra Garra, Jingurudó (MHCH3042, Fig. 8C): Dorsal colour Flesh (249) with Warm Sepia (40) irregular blotches and spots; Warm Sepia (40) interorbital band; upper surface of thigh with Warm Sepia (40) bars; groin and posterior surface of thigh suffused with Geranium (66); upper and lower iris region Olive Horn (16), iris centre Walnut Brown (27); iris periphery Jet Black (300); eye periphery Smoky White (261).

Ambroya, Maje (specimen not collected, Fig. 9A): Dorsal colour Chamois (84) with small Warm Sepia (40) spots; iris Spectrum Red (67); iris periphery Jet Black (300); eye periphery Smoky White (261). Chucanti, SMF50945 (Fig. 9B), dorsal colour Chesnut (30) with some Dusky Brown (285) blotches; dorsolateral line from the tip of snout to the groin Flesh (249); lateral colour Salmon (58); upper surface of thigh with Dusky Brown (285) bars; groin and posterior surface of thigh Flame Scarlet (73); upper and lower iris region Spectrum Red (67); iris periphery Jet Black (300); eye periphery Light Lavender (201). Chucanti, MHCH3043 (Fig. 9C), dorsal colour Deep Vinaceous (248) with the frontal region in Pale Pinkish Buff (3); groin and posterior surface of thigh Flame Scarlet (73); iris Spectrum Red (67); iris periphery Jet Black (300); eye periphery Light Lavender (201).

Chucanti (specimen not collected, Fig. 9D), dorsal colour Clay (18) with a dorsolateral line from the tip of snout to the groin in Cream (12); groin and posterior surface of thigh Flame Scarlet (73); iris Pale Neutral Gray (296); iris periphery Jet Black (300); eye periphery Light Lavender (201).